

1 **Single-cell quantitative bioimaging of *P. berghei* liver stage translation.**

2 James L. McLellan<sup>1</sup>, William Sausman<sup>1</sup>, Ashley B. Reers<sup>2</sup>, Evelien M. Bunnik<sup>2</sup>, Kirsten K. Hanson<sup>1,3</sup>

3

4 <sup>1</sup>Department of Molecular Microbiology and Immunology and South Texas Center for Emerging Infectious  
5 Diseases, University of Texas at San Antonio, San Antonio, TX, USA

6 <sup>2</sup>Department of Microbiology, Immunology, and Molecular Genetics, Long School of Medicine, University  
7 of Texas Health Science Center, San Antonio, TX, USA

8 <sup>3</sup>Corresponding author

9

10

11 **ABSTRACT**

12

13 *Plasmodium* parasite resistance to existing antimalarial drugs poses a devastating threat to the  
14 lives of many who depend on their efficacy. New antimalarial drugs and novel drug targets are in  
15 critical need, along with novel assays to accelerate their identification. Given the essentiality of  
16 protein synthesis throughout the complex parasite lifecycle, translation inhibitors are a  
17 promising drug class, capable of targeting the disease-causing blood stage of infection, as well  
18 as the asymptomatic liver stage, a crucial target for prophylaxis. To identify compounds capable  
19 of inhibiting liver stage parasite translation, we developed an assay to visualize and quantify  
20 translation in the *P. berghei*-HepG2 infection model. After labeling infected monolayers with o-  
21 propargyl puromycin (OPP), a functionalized analog of puromycin permitting subsequent  
22 bioorthogonal addition of a fluorophore to each OPP-terminated nascent polypeptide, we use  
23 automated confocal feedback microscopy followed by batch image segmentation and feature  
24 extraction to visualize and quantify the nascent proteome in individual *P. berghei* liver stage

25 parasites and host cells simultaneously. After validation, we demonstrate specific,  
26 concentration-dependent liver stage translation inhibition by both parasite-selective and pan-  
27 eukaryotic active compounds, and further show that acute pre-treatment and competition  
28 modes of the OPP assay can distinguish between direct and indirect translation inhibitors. We  
29 identify a Malaria Box compound, MMV019266, as a direct translation inhibitor in *P. berghei*  
30 liver stages and confirm this potential mode of action in *P. falciparum* asexual blood stages.

31

## 32 **Introduction**

33

34 *Plasmodium* parasites are the causative agent of malaria and continue to have an outsized effect on  
35 global public health, causing an estimated 241 million cases in 2020, with 77% of deaths occurring in  
36 children under the age of five (1). Antimalarial drugs are essential for treating malaria, however, all  
37 currently used antimalarials are associated with parasite resistance. The spread of *kelch13*-mediated  
38 resistance to the front-line antimalarial artemisinin in South East Asia and its recent *de novo* emergence  
39 in Rwanda demonstrate the critical threats to the efficacy of artemisinin combination therapies (ACTs),  
40 the front-line therapeutics targeting asexual blood stage (ABS) parasites, which cause all malaria  
41 symptoms (2-5). In addition to treating malaria, antimalarial drugs would ideally be able to clear any  
42 non-replicative gametocytes in the blood, preventing transmission back to the mosquito vector.  
43 Antimalarials are also crucial for disease prophylaxis, with the *Plasmodium* liver stage a key target to  
44 prevent both disease and transmission (6). Attractive antimalarials would thus have activity against each  
45 of these 3 stages despite significant stage-specific differences in biology (7-9), highlighting the utility of  
46 targeting core cellular processes, like translation, that are crucial for all mammalian stages of  
47 development.

48

49 Translation of mRNA nucleotide sequences to amino acids during the ribosomal synthesis of  
50 proteins is a central evolutionarily conserved cellular process that has been extensively targeted with  
51 antibiotics treating bacterial infections (10), but *Plasmodium* translation has not been targeted by any  
52 clinically approved antimalarials to date. *Plasmodium* protein synthesis is a highly desirable process to  
53 target, as translation can be blocked via many different molecular targets. DDD107498 (also known as  
54 cabamiquine and M5717), which is thought to target eEF2, a core component of polypeptide elongation  
55 on the ribosome (11), and a number of cytoplasmic aminoacyl-tRNA synthetase (aaRS) inhibitors, which  
56 prevent the linkage between a tRNA and its cognate amino acid, are in various stages of clinical and pre-  
57 clinical development, respectively (12, 13). Additionally, many pan-eukaryotic translation inhibitors have  
58 antiplasmodial activity against *P. falciparum* (Pf) ABS in standard 48 hour (h) assays, and were shown to  
59 directly target the Pf cytoplasmic translation apparatus using a bulk ABS lysate approach in which  
60 translation of the exogenous luciferase transcript is used as a biomarker for total cellular translation (14,  
61 15). Currently, the ability to gain such mechanistic information about antimalarial activity is almost  
62 entirely dependent on ABS experiments (16), with the assumption that antiparasitic activity in other  
63 stages occurs via the same mechanism. Liver stages are particularly problematic as they rely on highly  
64 metabolically active hepatocytes for their own development, which makes bulk population readout of  
65 conserved processes like translation impossible due to the signal from hepatocytes themselves. It also  
66 complicates interpretation of liver stage antiplasmodial activity, as it may integrate both hepatocyte-  
67 and parasite-directed effects.

68

69 Here, we report a bioimage-based assay quantifying *P. berghei* liver stage translation in the native  
70 cellular context. We rely on the activity of the aminoacyl-tRNA mimic puromycin, which is covalently  
71 bound to the C-terminus of a nascent polypeptide during the elongation reaction, causing the ribosome

72 to disassociate and release the puromycin-bound nascent-polypeptide (17-21). A synthetic puromycin  
73 analog, puromycin (OPP), was shown to truncate and label nascent polypeptides in an identical manner,  
74 but contains a small alkyne tag, facilitating the copper-catalyzed cycloaddition of a picolyl azide  
75 fluorophore in a bioorthogonal reaction, commonly termed “click chemistry” (22). Combining the OPP  
76 labeling of nascent polypeptides with automated fluorescence microscopy and quantitative image  
77 analysis, we demonstrate specific and separable *in cellulo* quantification of *P. berghei* and *H. sapiens*  
78 translation during liver stage development in HepG2 cells, and use the assay to identify both direct and  
79 indirect inhibitors of *Plasmodium* liver stage translation.

80

## 81 **Results**

82

### 83 **Visualization of the *Plasmodium* nascent proteome.**

84 With a goal of quantifying translation in single parasites, we first explored whether OPP would  
85 label the *P. berghei* nascent proteome during liver stage development. Infected HepG2 cells were  
86 treated with OPP for 30 minutes at 37°C, then immediately fixed with 4% paraformaldehyde, which  
87 stops the labeling reaction and preserves the quantity and cellular localization of the OPP-labeled  
88 polypeptides (22). Post-fixation, a click chemistry reaction attaches a picolyl azide conjugated  
89 fluorophore to the OPP-labelled polypeptides of both host and parasite, which can then be visualized  
90 with fluorescence microscopy. AlexaFluor555 was used to visualize newly synthesized peptides  
91 throughout this study, and the resulting signal, from both host and parasite nascent proteomes, will be  
92 referred to as OPP-A555. As expected, we can visualize translation throughout liver stage parasite  
93 development (Fig. 1A), from newly invaded sporozoite (2 hpi), through merozoite formation (57 hpi). By  
94 eye, parasite translation intensity (evidenced by OPP-A555 signal) appears generally greater than that of  
95 the host cell and surrounding non-infected HepG2 cells. The robust and highly specific OPP-A555 signal

96 (Fig. S1) suggests that this approach can be adapted to directly quantify translation of the intrahepatic  
97 parasite. The OPP labeling technology is particularly flexible, as it does not require any genetic  
98 modifications to label the nascent proteome and should thus be directly adaptable to a wide variety of  
99 organisms, including other *Plasmodium* species and stages. Supporting this, *P. falciparum* asexual blood  
100 stage translation can also be visualized in infected erythrocytes using a highly similar protocol (Fig. S2).

101 OPP labeling of nascent polypeptides requires active protein synthesis and should be responsive  
102 to chemical inhibition of translation prior to OPP labeling. Treatment of infected HepG2 cells with pan-  
103 eukaryotic or *Plasmodium*-specific translation inhibitors recapitulated known inhibitor specificity.  
104 Acute treatment with cycloheximide, which blocks translation elongation via binding the ribosomal E-  
105 site (23) and is active against both human and *Plasmodium* translation (24, 25), results in loss of the  
106 OPP-A555 signal, indicating a dramatic drop in protein synthesis of both HepG2 and parasite (Fig. 1B).  
107 DDD107498 is a *Plasmodium*-specific translation inhibitor thought to target eEF2 (11), and treatment  
108 results in loss of OPP-A555 signal only in the parasite, with host HepG2 and parasite nascent proteome  
109 (OPP-A55 signal) clearly separable with confocal microscopy (Fig. 1B, S3). Taken together, our data  
110 suggest that OPP labeling of the nascent proteome will allow separate quantification of *Plasmodium*  
111 liver stage translation and that of the host HepG2 cells, thus opening up the study of chemical inhibitors  
112 of translation beyond the *Plasmodium* asexual blood stage.

113

#### 114 **Quantification of the *P. berghei* and HepG2 nascent proteomes.**

115 To move from visualization to quantification of the nascent proteome, we utilized automated  
116 confocal feedback microscopy (ACFM) (26) to generate unbiased confocal image sets of single *P. berghei*  
117 liver stage parasites and the HepG2 cells immediately surrounding them (referred to as in-image  
118 HepG2). Image sets consisted of 3 separately acquired channels with anti-HSP70 marking the

119 exoerythrocytic parasite forms (EEFs), Hoechst-labeled DNA, and OPP-A555 labeling the nascent  
120 proteome in both HepG2 and EEF. We established a CellProfiler (27) pipeline for batch image processing,  
121 in which an EEF object segmented in the anti-HSP70 image was then used to mask the other two images  
122 for further segmentation and feature extraction (Fig. S4), including fluorescence intensity metrics  
123 describing the magnitude of parasite translation via the OPP-A555 signal. To quantify the in-image  
124 HepG2 nascent proteome regardless of OPP-A555 signal intensity, we used segmented HepG2 nuclei  
125 from the Hoechst image to define the pixels within which to quantify OPP-A55, as this measurement is  
126 tightly correlated ( $R = 0.94$ ) with the full cellular HepG2 OPP-A555 signal in control images (Fig. S5). With  
127 an image segmentation and feature extraction pipeline in place, we returned to OPP-A555 labeling  
128 controls to establish the detectable range of signal specific to the nascent proteome in both *P. berghei*  
129 EEFs and in-image HepG2 cells. Infected cells that received no OPP, but were subjected to a click labeling  
130 reaction with A555, had a larger signal than those which were OPP labeled without fluorophore  
131 conjugation. Both were extremely small, though, relative to the specific signal from parasite and HepG2  
132 nascent proteomes, allowing us to specifically quantify translation over a range of  $\geq 3$  log units (Fig. S6).

### 133 **Assessing liver stage translation inhibition by compounds with diverse mechanisms of action.**

134 Having established a robust assay to quantify the *P. berghei* LS nascent proteome, we next  
135 tested a select set of compounds including 9 antimalarials and 10 pan-eukaryotic bioactive compounds  
136 for their ability to inhibit *P. berghei* LS translation. The pan-eukaryotic actives include 7 compounds that  
137 are known translation inhibitors and 3 compounds with different mechanisms of action (Table S1). While  
138 all the pan-eukaryotic compounds have demonstrated antiplasmodial activity against *P. falciparum*  
139 asexual blood stages in either growth or re-invasion assays where compounds are present throughout  
140 48+ hours (28-34), comparable data for their liver stage activity cannot be generated due to the  
141 confounding effects that such compounds have on HepG2 cell viability (Fig. S7). To avoid confounding

142 effects of long term treatment, we first tested compounds for ability to inhibit *P. berghei* LS translation  
143 after an acute pre-treatment of 3.5 h followed by 30 minutes of OPP labeling in the continued presence  
144 of test compound (Fig. 2A). Each of the 19 compounds were tested at micromolar concentrations  
145 expected to be saturating, but which did not induce visible HepG2 toxicity, such as cell detachment or  
146 rounding up during 4 h (Table S1). 6 of the 7 pan-eukaryotic translation inhibitors tested inhibited *P.*  
147 *berghei* LS translation by  $\geq 90\%$ , and, as expected, the same 6 translation inhibitors reduced HepG2  
148 translation by  $\geq 90\%$  (Fig. 2B). In contrast, treatment with the threonyl-tRNA synthetase inhibitor  
149 borrelidin (35, 36) caused only a 53% mean reduction *P. berghei* LS translation and an 88% mean  
150 reduction in HepG2 translation (Fig. 2B). Differences in efficacy of human and *Plasmodium* translation  
151 inhibition were also detected for several other compounds. Halofuginone, an inhibitor of *P. falciparum*  
152 prolyl-tRNA synthetase (37), and emetine, which inhibits *P. falciparum* elongation (38), both displayed  
153 greater efficacy against HepG2 than *P. berghei*, while cycloheximide was slightly more effective against  
154 the parasite (Fig. 2B). Bruceantin, a translation initiation inhibitor (39), and the elongation inhibitors  
155 anisomycin and lactimidomycin (23) caused similar levels of translation inhibition between *P. berghei*  
156 and HepG2 cells (Fig. 2B).

157 To probe assay specificity, we tested three compounds known to be highly active against HepG2 and  
158 *Plasmodium* with cellular modes of action other than translation inhibition, which lead to complete  
159 HepG2 toxicity within 48 hours (Fig. S7). Surprisingly, the 26S proteasome inhibitor bortezomib (40)  
160 caused an 86% reduction in *P. berghei* liver stage translation, but had little effect on HepG2 translation  
161 (Fig. 2C). Trichostatin A, a histone deacetylase inhibitor (41), and Brefeldin A, which blocks the secretory  
162 pathway in *P. berghei* LS and *P. falciparum* ABS (42, 43) inhibited liver stage translation by 44% and 46%  
163 respectively (Fig. 2C and Table S1). The third group of test compounds consisted of known antimalarials,  
164 with all but mefloquine known to be active against *Plasmodium* liver stages (44). None of these  
165 antimalarials affected HepG2 translation following acute pre-treatment (Fig. 2D), but two substantially

166 reduced liver stage translation. DDD107498 (cabamiquine, M5717), thought to act via eEF2 inhibition  
167 and a known translation inhibitor in *P. falciparum* ABS (11) inhibited liver stage translation by 86% (Fig.  
168 2D). KAF156 (Ganaplacide), thought to affect the secretory pathway at the level of the ER or Golgi (45,  
169 46), was unexpectedly active in the assay, reducing mean *P. berghei* translation by 76% (Fig. 2D). Three  
170 antimalarial compounds caused only slight decreases in *P. berghei* translation following a 3.5 h acute  
171 pre-treatment, including atovaquone, which targets the bc1 complex (47), DSM265, a *Plasmodium*  
172 DHODH inhibitor (48), and MMV390048, which targets *Plasmodium* PI4K (49). The remaining  
173 antimalarial compounds had little or no on parasite translation and included *Plasmodium* DHFR  
174 inhibitors pyrimethamine (50) and P218 (51), the 8-aminoquinolone tafenoquine, which lacks a clear  
175 mechanism (52), and mefloquine, thought to target *Plasmodium* blood stage feeding but also proposed  
176 to inhibit the ribosome (53, 54).

177 All compounds inhibiting *P. berghei* or HepG2 translation by at least 50% were considered active, and  
178 progressed to concentration-response analysis.

179 We initially chose to run the acute pre-treatment assay during late schizogony due to the  
180 advantages of imaging larger parasites, but found that a substantial number of control parasites had  
181 translational outputs resembling those pre-treated with translation inhibitors (Fig. 2). Given that all  
182 *Plasmodium* LSs do not successfully complete development *in vitro* (55, 56), we performed the  
183 concentration-response experiments during both early and late schizogony in parallel (Fig. 3A) to  
184 additionally probe for developmental differences in parasite translation. Using 11 paired datasets, raw  
185 mean translation intensity in 28 vs. 48 hpi parasites was significantly different while that of in-image  
186 HepG2 was not ( $p=0.00019$  (LS),  $0.0995$  (HepG2); paired t-test). We defined individual parasites as  
187 “translationally impaired” if the OPP-A555 MFI was  $\leq 50\%$  of the mean OPP-A555 of all in-plate DMSO  
188 controls, and similarly classified the in-image HepG2. Using this definition of translational impairment,  
189 there is a substantial increase in translationally impaired control LSs at 48 hpi (33.3%) vs. 28 hpi (7.7%),

190 while a more modest shift was seen in the HepG2 (Fig. 3B). On average, parasite size was highly similar  
191 between translationally impaired and unimpaired parasites at 28 hpi, but markedly different at 48 hpi  
192 (Fig. S8  $p < 0.005$ ), suggesting that translational impairment at 48 h control parasites is indicative of  
193 earlier developmental failure or growth inhibition.

194         Despite the marked difference in translational heterogeneity between the parasite populations  
195 at 28 and 48 hpi, both efficacy and potency of the 10 compounds active against liver stage protein  
196 synthesis were quite similar in early vs. late schizogony, reproducible across independent experiments  
197 (Figs. 3C, S9, S10). Anisomycin, which blocks elongation by occupying the A-site and preventing peptide  
198 bond formation (23, 57), has very similar potency against human and *P. berghei* translation, while  
199 DDD107498 is completely parasite-specific, as expected (Fig. 3D). Modest selectivity towards *P. berghei*  
200 is seen for bruceantin, the most potent inhibitor tested, while emetine has greater potency against  
201 HepG2 protein synthesis (Fig. 3D, S9, S10). For all pan-eukaryotic translation inhibitors tested except  
202 borrelidin, which only achieved 64% inhibition at the maximum concentration tested against early LSs,  
203 translation inhibition efficacy was similar between HepG2 and *Plasmodium* (Fig. 3D, S9, S10).  
204 Lactimidomycin lost potency against both *Plasmodium* and HepG2 translation during late schizogony  
205 (Figs. 3C, S9, S10); this likely reflects compound instability (see Methods). Anisomycin, bruceantin,  
206 cycloheximide, halofuginone, and lactimidomycin all inhibited protein synthesis in early liver stage  
207 schizonts by  $> 95\%$  (Table S2) after 3.5 h of treatment, despite their varied modes/mechanisms of  
208 action. DDD107498, reached only 90.5% inhibition with the same treatment duration at the highest dose  
209 tested, despite having clearly achieved a saturating response (Fig. 3D, Table S2). Concentration-  
210 dependent inhibition of LS translation was seen for both KAF156 and bortezomib, which reached 77%  
211 and 86% inhibition, respectively (Table S2).

212 **Differentiating between direct and indirect inhibitors of *Plasmodium* translation.**

213           The acute pre-treatment assay was designed to maximize signal from translation inhibitors while  
214 avoiding confounding effects from HepG2 toxicity often seen with long treatment windows. However,  
215 this means that the assay should identify both direct protein synthesis inhibitors, and those that inhibit  
216 translation indirectly, e.g. compounds that induce cellular stress, leading to a signaling-based shutdown  
217 of protein synthesis via phosphorylation of eIF2 $\alpha$  (58). To test whether our 10 active compounds are  
218 direct or indirect translation inhibitors, we ran a competition OPP assay (co-OPP), where OPP and the  
219 compound of interest are added to *P. berghei*-infected HepG2 monolayers concomitantly. Since  
220 puromycin analogues like OPP truncate a nascent polypeptide chain at the position they are  
221 incorporated, the co-OPP assay effectively means there is direct competition between the test  
222 compound and OPP to shut down translation of each nascent polypeptide at each codon (17, 20-22).  
223 Direct translation inhibitors will reduce OPP-A555 labeling of the nascent proteome competitively, while  
224 indirect translation inhibitors are expected to be inactive, or with reduced activity, in the co-OPP assay.

225           The co-OPP assay was first run at top concentration (see Table S1) during both early and late *P.*  
226 *berghei* schizogony. Strikingly, both KAF156 and bortezomib, the two unexpected actives in acute pre-  
227 treatment mode, were not competitive inhibitors of OPP labeling at either timepoint, and are thus  
228 indirect translation inhibitors (Fig. 4A-B). Here, bortezomib treatment increased translational intensity  
229 in HepG2 cell at both time points and in early *P. berghei* schizonts (Fig. 4A-B and Table S2). Anisomycin,  
230 bruceantin, cycloheximide, emetine, halofuginone, and lactimidomycin were all direct inhibitors of both  
231 *P. berghei* and HepG2 protein synthesis, while DDD107498 was a direct inhibitor of parasite translation  
232 only (Fig. 4A-B). Anisomycin and DDD107498, thought to act against the elongation step of protein  
233 synthesis, and bruceantin, which inhibits translation initiation, were selected for 5pt. 10-fold serial  
234 dilution dose response to test whether any difference in potency could be detected in co-OPP versus  
235 acute pre-treatment assays in early *P. berghei* liver stage schizonts. Bruceantin showed a clear reduction  
236 in parasite translation inhibition potency in the competition assay, with a ~6-fold shift in EC<sub>50</sub>, while

237 DDD107498 and anisomycin did not (Fig. 4C and Table S2). The success of the competition assay in  
238 identifying all known direct inhibitors of HepG2 translation, and the demonstration that these pan-  
239 eukaryotic actives are similarly direct translation inhibitors in *P. berghei* EEFs suggests that the co-OPP  
240 assay can be useful to identify unknown translation inhibitors in primary or secondary screens.

241

#### 242 **Investigation of the mechanism of indirect translation inhibition by bortezomib and KAF156.**

243 Our finding that bortezomib and KAF156 similarly caused indirect translation inhibition in *P.*  
244 *berghei* LSs was unexpected, as they have distinct modes of action. They may, however, converge  
245 phenotypically downstream of ER stress, as bortezomib-driven accumulation of misfolded or damaged  
246 proteins in the ER causes an unfolded protein response (UPR) that is partially conserved in *Plasmodium*  
247 (59), while multiple lines of evidence indicate that KAF156 affects the parasite ER (45, 60). To investigate  
248 whether ER stress might be driving the indirect translation inhibition caused by KAF156 and bortezomib,  
249 we first investigated the phenotypic impact of both compounds on *P. berghei* LS ER structure using BiP,  
250 an HSP70 localized to the ER lumen (61), as a marker in immunofluorescence analysis (IFA). The LS  
251 schizont ER is a single, continuous structure composed of ER centers (tight accumulations of tubules)  
252 interconnected by a network of thin tubules (62) (Fig. 5A, DMSO). A 4h brefeldin A (BFA) treatment  
253 causes these centers to collapse into a single structure while the immunofluorescence intensity of anti-  
254 BiP labeling is similar to the control; DDD107498 treatment led to a similar collapse of ER centers,  
255 together with a substantial reduction in BiP IFA signal intensity localized to a single dim ER center (Fig.  
256 5A). Bortezomib and KAF156 both altered the ER morphology profoundly, with the ER appearing to have  
257 fragmented or vesiculated throughout the EEF (Fig. 5A). Strikingly, bortezomib also caused a marked  
258 reduction in BiP signal intensity, like DDD107948, while KAF156 does not (Fig. 5A). These findings  
259 support the hypothesis that KAF156 and bortezomib could both induce ER stress leading to subsequent  
260 translational arrest in the PbLS.

261           The *Plasmodium* response to ER stress appears to lack the transcriptional regulatory arm of the  
262 eukaryotic UPR (62, 63), but that which attenuates translation via eIF2 $\alpha$  phosphorylation is present and  
263 active. Three eIF2 $\alpha$  kinases exist in *Plasmodium* (64), with PK4 (PBANKA\_1126900, PF3D7\_0628200)  
264 mediating phosphorylation of eIF2 $\alpha$  when ER stress is induced by DTT or artemisinin in *P. berghei* and *P.*  
265 *falciparum* asexual blood stages (65-67). *Plasmodium* PK4 appears orthologous to the human PERK  
266 kinase, and *P. falciparum* and *P. berghei* PK4 activity can be inhibited by the human PERK inhibitor  
267 GSK2606414 (PK1) (65, 66, 68). To test whether indirect translation inhibition caused by bortezomib and  
268 KAF156 was mediated by the eIF2 $\alpha$  kinase PK4, we tested if PK1 pre-treatment could prevent translation  
269 inhibition by these compounds. DDD107498 was used as a control, since it inhibits *P. berghei* LS  
270 translation directly (Fig. 4), and PK4 inhibition should thus have no effect on its activity. We first tested  
271 4-hour PK1 pre-treatment at 0 (DMSO control), 2 or 10  $\mu$ M from 20-24 hpi, followed by the addition of  
272 KAF156 (0.5  $\mu$ M), bortezomib (1  $\mu$ M), DDD107498 (0.1  $\mu$ M) or DMSO from 24-28 hpi, with OPP added in  
273 the final 30 minutes. These concentrations of KAF156, bortezomib and DDD107498 were chosen to  
274 induce sub-maximal translation inhibition, and showed clear, but incomplete reduction in the OPP-A555  
275 median fluorescence intensity in single parasites (Fig. 5B). However, pre-treatment with PK1 did not  
276 prevent subsequent inhibition of EEF translation by bortezomib, KAF156, or DDD107498 (Fig. 5B). We  
277 also tested a shortened 20  $\mu$ M PK1 pre-treatment and shortened KAF156 and bortezomib treatments,  
278 as prolonged PK1 treatment at this concentration leads to HepG2 cytotoxicity (not shown). Control  
279 experiments demonstrate that 2 h treatments with bortezomib or KAF156 are sufficient to induce  
280 translational arrest, but once again, PK1 was not able to prevent translation inhibition by either  
281 compound (Fig. 5C). In both PK4 inhibition protocols, in-image HepG2 translation was also quantified.  
282 Bortezomib treatment alone led to a reduction in HepG2 translation as has been previously  
283 demonstrated, and shown to be mediated by human PERK (69); PERK inhibition by PK1 pre-treatment  
284 markedly increased HepG2 translation after addition of bortezomib (Fig. S11). These results

285 demonstrate that the indirect translation inhibition induced by KAF156 and bortezomib is not mediated  
286 by *Plasmodium* PK4. Another hypothesis for this indirect translation inhibition is that it reflects a rapid  
287 parasite death process. If so, the translation inhibition should not be reversible. We tested this directly  
288 by comparing reversibility of the translation inhibition induced by 4 h KAF156 and anisomycin  
289 treatments in early schizogony. Anisomycin-induced translation inhibition is reversible in human cells  
290 (57), and the ~95% inhibition of *P. berghei* liver stage translation was completely reverted 20h after  
291 compound washout (Fig. 5D). KAF156 treatment induced weaker translation inhibition (~85%)  
292 compared to anisomycin but showed very little recovery of translation 20 h after washout. The  
293 irreversibility of the translation inhibition after washout suggests that KAF156 treatment causes rapid  
294 parasite death.

295

296 **Testing uncharacterized *P. berghei* liver stage active compounds for the ability to inhibit protein**  
297 **synthesis.**

298 Finally, to investigate the utility of this assay for identifying novel *Plasmodium* protein synthesis  
299 inhibitors, we tested 6 compounds from the MMV Malaria Box that are active against *P. berghei* liver  
300 stages and phenotypically similar to DDD107498 in 48h luciferase assays (70). Acute pre-treatment with  
301 MMV019266 reduced EEF translation by 87% (Fig. 6A). The remaining compounds were much less  
302 active, with MMV665940, MMV007116, and MMV006820 causing roughly 30% reduction in PbLS  
303 translation, MMV006188 causing a 19% reduction, and MMV011438 having no effect (Fig. 6A).  
304 MMV019266 similarly inhibited LS translation at both 1 and 10  $\mu$ M during early and late schizogony  
305 (Figs. 6B-C, S12, Table S2). MMV019266 had EC<sub>50</sub> values of 373 and 289 nM at 28- and 48 hpi,  
306 respectively in the acute pre-treatment assay (Fig. S12 and Table S2). MMV019266 was also capable of  
307 inhibiting *P. falciparum* ABS translation in intact schizonts, with the degree of inhibition similar to that

308 seen with 10  $\mu$ M DDD107498, but greater than 20 nM DDD107498 and less than 100 nM bruceantin  
309 (Fig. S13). The co-OPP assay demonstrated that MMV019266 is a direct protein synthesis inhibitor,  
310 causing 77% and 72% reductions in PbLS translational intensity during early and late schizogony  
311 respectively (Fig. 6D and Table S2). Identification of MMV019266 as a direct translation inhibitor in both  
312 blood stage and liver stage parasites highlights the utility of the *P. berghei* LS OPP assay to antimalarial  
313 drug discovery.

314

## 315 **Discussion**

316 Our results demonstrate the feasibility and utility of single cell image-based quantification of  
317 protein synthesis in an intracellular parasite that resides in a translationally active host cell, and open up  
318 the study of *Plasmodium* liver stage translation for drug discovery applications and in the native  
319 developmental context. To date, studies of the mode of action and target of antimalarial compounds  
320 largely rely on studies in *P. falciparum* asexual blood stages (ABS), with the assumption that it will be the  
321 same in other stages and species in which a compound has antiplasmodial activity. Molecular targets of  
322 antimalarials compounds have been identified and validated in *P. falciparum* ABS through *in vitro*  
323 evolution of drug resistance, cellular thermal shift assays, chemoproteomics, metabolic profiling, and a  
324 variety of reverse genetics approaches to produce modified parasite lines (71-74). Re-use of these same  
325 evolved or genetically modified parasite lines, metabolic profiling and assays quantifying intracellular  
326 ionic concentrations all support further understanding of antimalarial compound modes of action in ABS  
327 (75-77). Protein synthesis in ABS has long been quantified by feeding with radiolabelled amino acids and  
328 more recently *P. falciparum* ABS lysate assays detecting the translation of a single model transcript  
329 encoding a luciferase enzyme have been used to screen several small compound libraries and  
330 characterize the activity of known pan-eukaryotic translation inhibitors (14, 15, 78).

331 An overarching difficulty in quantification of conserved biochemical or cellular processes like  
332 protein synthesis in *Plasmodium* liver stages is the dominant contribution of hepatocytes to any signal  
333 from an infected monolayer. In ABS, this problem is easily overcome, as saponin lysis of infected RBC  
334 cultures has long been recognized to allow parasite purification (79), and mature human erythrocytes  
335 lack most core cellular processes, e.g. protein synthesis, allowing *Plasmodium* translation to be  
336 quantified directly in bulk ABS cultures or lysates. Inability to physically isolate liver stage parasites or  
337 isolate the parasite signal from that of the hepatocytes prevents the use of these approaches in  
338 *Plasmodium* liver stages currently. Here, we overcome this limitation by using computational separation  
339 of the combined fluorescent signal of the nascent proteome of infected HepG2 monolayers into  
340 separate *P. berghei* and hepatoma cells signals in ACFM-acquired image sets. The specificity of this  
341 approach is clear from *Plasmodium*-specific inhibition of translation by DDD107498, and our ability to  
342 detect differential inhibition of *H. sapiens* vs. *P. berghei* translation with pan-eukaryotic inhibitors like  
343 emetine and bruceantin means that both host and parasite nascent proteomes can be quantified in  
344 parallel, allowing determination of a compound's LS translation inhibition efficacy and selectivity in a  
345 single well. Similar quantitative bioimaging strategies may prove useful for drug discovery efforts with  
346 other eukaryotic parasites residing in translational active host cells.

347 One attractive feature of targeting *Plasmodium* translation is that such inhibitors would be  
348 predicted to have multistage activity, as has been demonstrated for DDD107498 and a variety of tRNA  
349 synthetase inhibitors ((11, 80). Though our data show that DDD107498 LS translation inhibition potency  
350 is 13-15 nM, clearly less than its ~1-2 nM LS antiparasmodial potency in standard 48 h LS biomass assays,  
351 it is clearly a concentration-dependent translation inhibitor. It is striking, though, that at 1 nM we detect  
352 no clear translation inhibition at all, and the slope is very shallow, with saturating effects only seen at  
353 1000 nM, and the percent max translation inhibition is clearly less than for other parasite-active  
354 compounds. These effects seem unlikely to be time dependent, as we show nearly identical

355 translational responses to DDD107498 in acute pre-treatment and co-OPP assays. Incomplete  
356 translation inhibition with saturating doses of DDD107498 was also seen in *P. falciparum* ABS (11), and it  
357 will be a future challenge to determine how much translation inhibition is required for DDD107498  
358 antiplasmodial activity. Consistent with the hypothesis that translation inhibitors should be multistage  
359 actives, we show concentration dependent LS inhibition for the elongation inhibitors anisomycin,  
360 lactimidomycin, emetine, and cycloheximide, the initiation inhibitor bruceantin, and the tRNA  
361 synthetase inhibitor halofuginone. Only borrelidin, a known inhibitor of threonyl-tRNA synthetase  
362 (ThrS) in both prokaryotes and eukaryotes (35), failed to show concentration dependent translation  
363 inhibition activity, and was only partially effective in our acute pre-treatment assay at the highest  
364 concentration tested (10  $\mu$ M), which is at odds with the low nanomolar antiplasmodial potency of  
365 borrelidin (29, 36, 81-83), where reported IC<sub>50</sub>s range from 0.07 nM to 1.9 nM. We tested borrelidin in a  
366 48h LS live luciferase assay, but all concentrations that reduced parasite biomass also showed effects on  
367 the HepG2 monolayer (data not shown), so it is unclear if borrelidin has any direct antiplasmodial  
368 activity against the *P. berghei* LS. Species specific differences in activity should not be the cause, as  
369 borrelidin was active against ABS of both human and murine *Plasmodium* spp., and was an effective  
370 antimalarial in murine infection models (29, 36, 81, 82). Furthermore, this disconnect is not easily  
371 explained by stage specific differences in the target enzyme expression or activity, as *Plasmodium*  
372 parasites encode only a single copy of ThrS (84), which is likely required for protein synthesis in both the  
373 cytoplasm and apicoplast (58, 85). Enzymatic evidence clearly shows that borrelidin is active against  
374 recombinant PfThrS *in vitro* (36), but the cellular evidence in support of borrelidin targeting *Plasmodium*  
375 ThrS was a modest shift in the *P. falciparum* ABS growth inhibition EC<sub>50</sub> when an excess of exogenous  
376 free L-threonine in growth media (81). Evolved *in vitro* resistance to borrelidin has not been reported to  
377 date. Given that compound efficacy against recombinant protein is not always a reliable indicator of *in*  
378 *vivo* antimalarial mechanism, as with triclosan (86), it will be important to clarify that ThrS is indeed the

379 relevant antimalarial target of borrelidin, and if so, understand why it is not effective against *P. berghei*  
380 liver stages *in vitro*.

381           The image-based OPP assay appears to have some advantages relative to the lysate assay, PfIVT,  
382 (14, 15, 78) in testing antiplasmodial compounds of unknown mechanism for translation inhibition  
383 activity. Given the liquid handling requirements for the OPP assay, it is ideally suited for use with  
384 adherent cells, and thus liver stage parasites, and while our current 96wp format is sufficient for testing  
385 of compounds of interest as we demonstrate here, we are miniaturizing the assay to 384wp format for  
386 medium throughput use. Image-based assays have the advantage of inherent ability to investigate  
387 ground-truth of translation inhibition metrics obtained via segmentation and feature extraction, as  
388 metadata links the original, unaltered image set to extracted features (87), while a lysate-based assay  
389 lacks inherent ground truth, and may require a secondary counterscreen to triage compounds against  
390 the translated reporter enzyme, as for PfIVT (78). Translation is a complex process, requiring spatial  
391 coordination of hundreds of gene products (58, 88) to produce new proteins from thousands of mRNAs,  
392 and the image-based OPP assay captures changes in output of the entire, native nascent proteome. A  
393 lysate-based assay using translation of a single exogenous mRNA as a readout reduces this complexity  
394 substantially, and may fail to identify compounds that active translation inhibitors *in cellulo*. Perhaps this  
395 occurred with MMV019266, which was not identified as an active compound in the PfIVT screen of the  
396 Malaria Box (14). We tested 6 compounds identified from the MMV Malaria Box as LS active with a 48h  
397 biomass assay phenotype indicative of early liver stage arrest (70), the same as for DDD107498, which  
398 we could source commercially. While 5 were inactive, the thienopyrimidine MMV019266 was identified  
399 as a direct translation inhibitor in *P. berghei* LS, and we demonstrated that it also inhibits *P. falciparum*  
400 translation in blood stage schizonts. MMV019266 is known to have antiplasmodial activity against a  
401 variety of species and life cycle stages, including *P. vivax* schizonts and *P. falciparum* gametocytes (70,  
402 89-93), and was predicted to target hemoglobin catabolism based on metabolic fingerprinting (94).

403 During the preparation of this manuscript, three related thienopyrimidines were reported to target the  
404 *P. falciparum* cytoplasmic isoleucyl tRNA synthetase (PfIIRS) based on mutations evolved *in vitro* in  
405 resistant lines and confirmed in conditional PfIIRS knockdowns and gene-edited parasite lines (95).  
406 These results highlight the value of the *P. berghei* liver stage OPP assay for identification of multistage  
407 *Plasmodium* translation inhibitors.

408 While our focus here has been using the quantitative image-based OPP assay to identify novel  
409 *Plasmodium* translation inhibitors and validate this mode of action in the liver stage for known inhibitors  
410 of *P. falciparum* blood stage translation, the flexibility of the assay and power of single cell data suggest  
411 it may prove quite useful in key applications beyond this. While our quantitative work utilized LS  
412 schizonts, we demonstrated specific nascent proteome signal in sporozoites through to monolayer  
413 merozoites, and intriguing changes in the subcellular localization of the nascent proteome seem to occur  
414 during *P. berghei* LS development. The difference in the fraction of translationally impaired parasites in  
415 28 vs. 48 hpi LS schizonts suggests that translational intensity may vary during liver stage development  
416 in populations, as it clearly does in individuals at both timepoints. Our identification of Kaf156 and  
417 bortezomib as indirect translation inhibitors not under the control of the eIF2 $\alpha$  kinase PK4, but likely  
418 causing rapid killing of *P. berghei* LS schizonts, indicates the potential of using translational output as a  
419 biomarker for liver stage parasite viability, something that remains lacking in the liver stage toolkit (96).  
420 The labeling protocol adapts easily to *P. falciparum* blood stages, as we demonstrate, though  
421 throughput is limited by the non-adherent erythrocytes, which also complicates high content  
422 quantitative imaging. While the throughput problem will be challenging to solve for medium to high  
423 throughput drug discovery, flow cytometry may be better suited to quantification of translation  
424 inhibition in based on fluorescent labeling of the *P. falciparum* nascent proteome, as has recently been  
425 done to characterize novel tyrosine-RNA synthetase inhibitors (97). As OPP labeling of the nascent  
426 proteome requires no transgenic technology, it should be readily adaptable to critical drug discovery

427 challenges such as testing target engagement and potency of translation inhibitors with diverse  
428 molecular mechanisms of action against field isolates of *P. falciparum* and *P. vivax*. Our quantitative  
429 bioimaging workflow should be repurposable for interrogation of translation inhibitors in *P. falciparum*  
430 and *P. vivax* liver stages and capable of integration into existing image based-screening platforms (98),  
431 and may have particular value in examining the role translation plays in formation of dormant  
432 hypnozoites and their reactivation.

433

## 434 **Materials and Methods**

### 435 **HepG2 culture and *P. berghei* sporozoite isolation and infection**

436 HepG2 human hepatoma cells were cultured in Dulbecco's Modified Eagle Medium (DMEM) (Gibco  
437 10313-021) supplemented with 10% (v/v) FBS, 1% (v/v) GlutaMAX (Gibco 35050-061), 1% (v/v) Penicillin-  
438 Streptomycin (Gibco 15140-122) and maintained at 37°C, 5% CO<sub>2</sub>. *Plasmodium berghei* sporozoites,  
439 expressing firefly luciferase-GFP fusion protein under the control of the exoerythrocytic form 1a (EEF1a)  
440 promoter (99), were isolated from the salivary glands of infected *Anopheles stephensi* mosquitos (NYU  
441 and UGA insectaries). Sporozoites were counted and diluted into infection DMEM (iDMEM) – cDMEM  
442 further supplemented with 1% (v/v) Penicillin-Streptomycin-Neomycin (Gibco 15640-055), 0.835µg/mL  
443 Amphotericin B (Gibco 15290-018), 500µg/mL kanamycin (Corning 30-006-CF), and 50µg/mL gentamycin  
444 (Gibco 15750-060), added to HepG2 monolayers, centrifuged at 3000 rpm for 5 minutes, and incubated  
445 in cell culture conditions for 2 hours before PBS washing and iDMEM replenishment for infections  
446 proceeding on glass coverslips. For infections in 96 well plates (Greiner 655098), infected HepG2  
447 monolayers were detached at 2 hpi using TrypLE Express (Gibco 12605-028), washed, counted, and re-  
448 seeded into 96 well plates.

449

### 450 **Compound handling and treatment**

451 Compound stocks prepared from powder were solubilized in DMSO (Sigma-Aldrich D2650), aliquoted,  
452 and stored at -20°C. For acute pre-treatments, infected cells were treated for 3.5 h prior to 30-minute  
453 OPP labeling in continued presence of compound. For coOPP assays, compound and OPP were applied  
454 simultaneously for 30 minutes. Concentration-response experiments were performed with 5 points in  
455 10-fold serial dilutions, and equimolar DMSO concentrations (0.001% v/v) were maintained across all  
456 treatments and controls. Compounds prepared in iDMEM were stored at 4°C and used within 24 h, e.g.  
457 a single dilution series was prepared and used for both the 24- & 44- hpi additions.

458

#### 459 **OPP labeling and fluorophore addition**

460 A 20 mM stock of O-propargyl puromycin (OPP) (Invitrogen C10459) in DMSO was diluted to label cells  
461 with 20 µM OPP for 30 mins at 37°C, according to the manufacturer's recommended protocol, before  
462 15-minute fixation with PFA (Alfa Aesar 30525-89-4) diluted to 4% in PBS. Copper-(I)-catalyzed  
463 cycloaddition of Alexafluor555 picolyl azide to OPP-labeled polypeptides was performed using Invitrogen  
464 Click-iT Plus AF555 (Invitrogen C10642) according to the manufacturer's recommendations, with a 1:4  
465 Cu<sub>2</sub>SO<sub>4</sub> to copper protectant ratio. 27µL of reaction mix was added to 96-wp wells, with 25 µL used for  
466 each glass coverslip, inverted on parafilm.

467

#### 468 **Immunofluorescence**

469 EEFs were immunolabeled using anti-PbHSP70 (2E6 mouse mAb) (100) (1:200), followed by donkey anti-  
470 mouse Alexafluor488 (Invitrogen A21202). In Fig. 1A, goat anti-UIS4 (Sicgen AB0042-500) (1:1000) was  
471 used to mark the newly invaded sporozoites, followed by donkey anti-goat 488 (Invitrogen A32814). To  
472 visualize the parasite ER in Fig. 5A, rabbit polyclonal anti-BiP (1:600, GenScript) serum, raised against the  
473 C terminal polypeptide CGANTPPPGDEDVDS from PBANKA\_081890 was used with donkey anti-rabbit  
474 Alexafluor555 (Invitrogen A31572) as the secondary. DNA was stained with Hoescht 33342 (Thermo

475 Scientific 62249) (1:1000). Antibodies were prepared in 2% BSA in PBS, with secondary antibodies used  
476 at a 1:500 dilution.

477

#### 478 ***Plasmodium falciparum* culture**

479 *P. falciparum* 3D7 parasites were cultured as previously described (101). In short, parasites were  
480 cultured in human AB<sup>+</sup> erythrocytes (Interstate Blood Bank, Memphis, TN, USA) at 3 – 10% parasitemia  
481 in complete culture medium (5% hematocrit). Complete culture medium consisted of RPMI 1640  
482 medium (Gibco #32404014) supplemented with gentamicin (45 µg/ml final concentration; Gibco  
483 #15710064), HEPES (40 mM; Fisher #BP3101), NaHCO<sub>3</sub> (1.9 mg/ml; Sigma #SX03201), NaOH (2.7 mM;  
484 Fisher #SS266-1), hypoxanthine (17 µg/ml; Alfa Aesar #A11481-06), L-glutamine (2.1 mM; Corning  
485 #25005Cl), D-glucose (2.1 mg/ml; Fisher #D16-1), and 10% (vol/vol) human AB<sup>+</sup> serum (Valley Biomedical  
486 #HP1022). Parasites were cultured at 37°C in an atmosphere of 5% O<sub>2</sub>, 5% CO<sub>2</sub>, and 90% N<sub>2</sub>.

487

#### 488 ***Plasmodium falciparum* blood stage immunofluorescence and OPP-A555 labeling**

489 *P. falciparum*-infected erythrocytes (iRBCs) in mixed culture were labeled using 20 µM OPP (Invitrogen  
490 C10459) at 37°C for 30 minutes, pelleted and washed with PBS before being resuspended in 1 mL of 4%  
491 PFA (Electron Microscopy Sciences 30525-89-4) + 0.0075% glutaraldehyde (Sigma G6257) in PBS for 30  
492 minutes at RT. Fixed iRBCs were pelleted and washed twice with PBS prior to permeabilization in 0.1%  
493 Triton X-100 (9002-93-1) in PBS for 10 minutes. Permeabilized iRBCs were washed twice in PBS, click-  
494 labeled as described for infected HepG2 monolayers, then pelleted, washed once with PBS and Hoechst-  
495 labelled for 30 minutes at RT. iRBCs were then pelleted, washed, and re-suspended in PBS before  
496 imaging.

497

#### 498 **HepG2 viability assay**

499 Non-infected HepG2 cells were treated with 10-point, 3-fold, serial dilutions with maximal  
500 concentrations of 10 $\mu$ M, except for cycloheximide (10 $\mu$ g/mL), GSK260414 (50 $\mu$ M), and emetine (25 $\mu$ M).  
501 At 46 hours post-treatment, AlamarBlue cell viability reagent (Invitrogen A50100) was applied at a 1X  
502 final concentration and incubated for one hour prior to measuring fluorescence at 590nm using a  
503 microplate reader (CLARIOstar, BMG LABTECH).

504

### 505 **Image acquisition**

506 Images were acquired on a Leica SP8 confocal microscope using an HC PL APO 63x/1.40 oil objective for  
507 glass coverslips and an HC PL APO 63x/1.40 water objective for 96-well  $\mu$ clear plates. Images in Figures  
508 1A, 5C, 7B, S1, S2, and S3 were acquired manually and processed using ImageJ (102). All other images,  
509 and all used for quantitative analysis, were acquired using automated confocal feedback microscopy  
510 (ACFM) (26). Briefly, MatrixScreener is used to define a patterned matrix for acquisition of non-  
511 overlapping, low-resolution images of the *P. berghei*-infected HepG2 monolayer. After each image is  
512 acquired, online image segmentation and ID of parasites, defined by PbHSP70 signal, is performed  
513 utilizing custom modules (<https://github.com/VolkerH/MatrixScreenerCellprofiler/wiki>) integrated into  
514 a CellProfiler version 2.0.11710 pipeline (27). The x-y coordinates of each parasite found are then used  
515 by MatrixScreener to sequentially image each individual parasite in high resolution, with an automated  
516 z-stack maximizing PbHSP70 intensity to identify the z coordinate, followed by sequential acquisition of  
517 Hoechst, PbHSP70, and OPP-A55 images. This process iterates until all parasites in the predefined matrix  
518 of the infected monolayer have been imaged.

519

### 520 **Image segmentation, feature extraction, and data cleaning**

521 Batch image segmentation and feature extraction were performed in Cell Profiler (v2.1.1 rev6c2d896)  
522 (27); see Fig. S4 for the workflow. Briefly, EEf objects were identified using a global Otsu segmentation

523 of the PbHSP70 image. The EEF object was shrunk by two pixels to ensure exclusion of HepG2-associated  
524 signal, and used to mask the OPP-A555 image to quantify *P. berghei* translation via OPP-A555  
525 fluorescence intensity features. Conversely, the EEF object was expanded by two pixels and used as an  
526 inverse mask for the Hoechst image to segment HepG2 nuclei. All in-image HepG2 nuclei were unified  
527 into a single object, then its OPP-A555 fluorescence intensity features were used to quantify HepG2  
528 translation. All features extracted were then analyzed using KNIME (103). ACFM image sets were  
529 computationally cleaned of image that did not contain a single true EEF in a HepG2 monolayer by  
530 removing data from those in which: more than one EEF object was identified, the EEF object identified  
531 did not contain a DNA signal, and no HepG2 nuclei were identified. EEF object form factor was used to  
532 identify rare instances of segmentation failure in which two parasites were segmented as a single EEF  
533 object; images sets corresponding to form factor outliers ( $> 1.5 \times \text{IQR}$ ) were visually inspected and  
534 removed if they did not contain a single, true EEF. Finally, focus score features for both the PbHSP70 and  
535 DNA images were used to exclude any image set where focus score  $< 1.5 \times \text{IQR}$ . Data cleaning was carried  
536 out per experiment, and resulted, on average, in the removal of 1.45% of the total data.

537

#### 538 **Concentration response curve fitting and statistics.**

539 Concentration-response analysis was performed using 4 parameter non-linear regression curve fitting in  
540 GraphPad Prism (Version 7.0d), with the top of the curve fixed at 100, and  $-10 < \text{hill slope} < 0$ . When  
541 maximal effect was reached with  $\geq 2$  concentrations tested, the bottom of the curve was fit open; if no  
542 such plateau was achieved, the curve was fit with maximal effect constrained to 0.  $\text{EC}_{50}$  and 95% CI were  
543 determined for each compound from  $\geq 3$  independent experiments. All other data and statistical  
544 analyses were performed in KNIME.

545

#### 546 **Data availability**

547 Image datasets are available upon request to the corresponding author.

548

549 **Acknowledgements**

550 This work was supported by National Institutes of Health grant R21AI149275 to KKH. JLM was supported  
551 by a South Texas Center for Emerging Infectious Diseases fellowship. ABR was supported by Graduate  
552 Research in Immunology Program training grant NIH T32 AI138944. We thank the New York University  
553 Insectary and the University of Georgia SporoCore for providing *P. berghei*-infected mosquitos. KKH  
554 conceived the project and designed experiments. JLM, WS, ABR, and KKH performed experiments. JLM  
555 and KKH analyzed the data. EMB and KKH supervised the work in their respective laboratories. JLM and  
556 KKH drafted the manuscript. All authors participated in review and editing of the manuscript, and  
557 approved the submitted version.

## 558 Works Cited

- 559 1. World Health Organization W. 2021. World malaria report 2021. World Health Organization,  
560 Geneva.
- 561 2. Blasco B, Leroy D, Fidock DA. 2017. Antimalarial drug resistance: linking Plasmodium falciparum  
562 parasite biology to the clinic. *Nature Medicine* 23:917-928.
- 563 3. Witkowski B, Khim N, Chim P, Kim S, Ke S, Kloeung N, Chy S, Duong S, Leang R, Ringwald P,  
564 Dondorp AM, Tripura R, Benoit-Vical F, Berry A, Gorgette O, Ariey F, Barale J-C, Mercereau-  
565 Puijalon O, Menard D. 2013. Reduced artemisinin susceptibility of Plasmodium falciparum ring  
566 stages in western Cambodia. *Antimicrobial agents and chemotherapy* 57:914-923.
- 567 4. Uwimana A, Legrand E, Stokes BH, Ndikumana J-LM, Warsame M, Umulisa N, Ngamije D,  
568 Munyaneza T, Mazarati J-B, Munguti K, Campagne P, Criscuolo A, Ariey F, Murindahabi M,  
569 Ringwald P, Fidock DA, Mbituyumuremyi A, Menard D. 2020. Emergence and clonal expansion of  
570 in vitro artemisinin-resistant Plasmodium falciparum kelch13 R561H mutant parasites in  
571 Rwanda. *Nature Medicine* 26:1602-1608.
- 572 5. Phillips MA, Burrows JN, Manyando C, van Huijsduijnen RH, Van Voorhis WC, Wells TNC. 2017.  
573 Malaria. *Nat Rev Dis Primers* 3:17050.
- 574 6. Burrows JN, Burlot E, Campo B, Cherbuin S, Jeanneret S, Leroy D, Spangenberg T, Waterson D,  
575 Wells TN, Willis P. 2014. Antimalarial drug discovery - the path towards eradication. *Parasitology*  
576 141:128-139.
- 577 7. Venugopal K, Hentzschel F, Valkiūnas G, Marti M. 2020. Plasmodium asexual growth and sexual  
578 development in the haematopoietic niche of the host. *Nature Reviews Microbiology* 18:177-189.
- 579 8. Prudêncio M, Rodriguez A, Mota MM. 2006. The silent path to thousands of merozoites: the  
580 Plasmodium liver stage. *Nature Reviews Microbiology* 4:849-856.
- 581 9. Matz JM, Beck JR, Blackman MJ. 2020. The parasitophorous vacuole of the blood-stage malaria  
582 parasite. *Nature Reviews Microbiology* 18:379-391.
- 583 10. Wilson DN. 2009. The A-Z of bacterial translation inhibitors. *Critical Reviews in Biochemistry and*  
584 *Molecular Biology* 44:393-433.
- 585 11. Baragana B, Hallyburton I, Lee MC, Norcross NR, Grimaldi R, Otto TD, Proto WR, Blagborough  
586 AM, Meister S, Wirjanata G, Ruecker A, Upton LM, Abraham TS, Almeida MJ, Pradhan A, Porzelle  
587 A, Luksch T, Martinez MS, Luksch T, Bolscher JM, Woodland A, Norval S, Zuccotto F, Thomas J,  
588 Simeons F, Stojanovski L, Osuna-Cabello M, Brock PM, Churcher TS, Sala KA, Zakutansky SE,  
589 Jimenez-Diaz MB, Sanz LM, Riley J, Basak R, Campbell M, Avery VM, Sauerwein RW, Dechering  
590 KJ, Noviyanti R, Campo B, Frearson JA, Angulo-Barturen I, Ferrer-Bazaga S, Gamo FJ, Wyatt PG,  
591 Leroy D, Siegl P, Delves MJ, Kyle DE, et al. 2015. A novel multiple-stage antimalarial agent that  
592 inhibits protein synthesis. *Nature* 522:315-20.
- 593 12. Pham JS, Dawson KL, Jackson KE, Lim EE, Pasaje CF, Turner KE, Ralph SA. 2014. Aminoacyl-tRNA  
594 synthetases as drug targets in eukaryotic parasites. *Int J Parasitol Drugs Drug Resist* 4:1-13.
- 595 13. Chhibber-Goel J, Yogavel M, Sharma A. 2021. Structural analyses of the malaria parasite  
596 aminoacyl-tRNA synthetases provide new avenues for antimalarial drug discovery. *Protein*  
597 *Science* 30:1793-1803.
- 598 14. Ah Yong V, Sheridan CM, Leon KE, Witchley JN, Diep J, DeRisi JL. 2016. Identification of  
599 Plasmodium falciparum specific translation inhibitors from the MMV Malaria Box using a high  
600 throughput in vitro translation screen. *Malar J* 15:173.
- 601 15. Sheridan CM, Garcia VE, Ah Yong V, DeRisi JL. 2018. The Plasmodium falciparum cytoplasmic  
602 translation apparatus: a promising therapeutic target not yet exploited by clinically approved  
603 anti-malarials. *Malaria Journal* 17:465.

- 604 16. Forte B, Otilie S, Plater A, Campo B, Dechering KJ, Gamo FJ, Goldberg DE, Istvan ES, Lee M,  
605 Lukens AK, McNamara CW, Niles JC, Okombo J, Pasaje CFA, Siegel MG, Wirth D, Wyllie S, Fidock  
606 DA, Baragaña B, Winzeler EA, Gilbert IH. 2021. Prioritization of Molecular Targets for  
607 Antimalarial Drug Discovery. *ACS Infectious Diseases* 7:2764-2776.
- 608 17. Azzam ME, Algranati ID. 1973. Mechanism of puromycin action: fate of ribosomes after release  
609 of nascent protein chains from polysomes. *Proceedings of the National Academy of Sciences of  
610 the United States of America* 70:3866-3869.
- 611 18. Barrett RM, Liu H-w, Jin H, Goodman RH, Cohen MS. 2016. Cell-specific Profiling of Nascent  
612 Proteomes Using Orthogonal Enzyme-mediated Puromycin Incorporation. *ACS Chemical Biology*  
613 11:1532-1536.
- 614 19. David A, Dolan BP, Hickman HD, Knowlton JJ, Clavarino G, Pierre P, Bennink JR, Yewdell JW.  
615 2012. Nuclear translation visualized by ribosome-bound nascent chain puromycylation. *The  
616 Journal of cell biology* 197:45-57.
- 617 20. Nathans D. 1964. PUROMYCIN INHIBITION OF PROTEIN SYNTHESIS: INCORPORATION OF  
618 PUROMYCIN INTO PEPTIDE CHAINS. *Proceedings of the National Academy of Sciences of the  
619 United States of America* 51:585-592.
- 620 21. Yarmolinsky MB, Haba GL. 1959. INHIBITION BY PUROMYCIN OF AMINO ACID INCORPORATION  
621 INTO PROTEIN. *Proceedings of the National Academy of Sciences of the United States of  
622 America* 45:1721-1729.
- 623 22. Liu J, Xu Y, Stoleru D, Salic A. 2012. Imaging protein synthesis in cells and tissues with an alkyne  
624 analog of puromycin. *Proc Natl Acad Sci U S A* 109:413-8.
- 625 23. Garreau de Loubresse N, Prokhorova I, Holtkamp W, Rodnina MV, Yusupova G, Yusupov M.  
626 2014. Structural basis for the inhibition of the eukaryotic ribosome. *Nature* 513:517-522.
- 627 24. Schneider-Poetsch T, Ju J, Eyler DE, Dang Y, Bhat S, Merrick WC, Green R, Shen B, Liu JO. 2010.  
628 Inhibition of eukaryotic translation elongation by cycloheximide and lactimidomycin. *Nat Chem  
629 Biol* 6:209-217.
- 630 25. Schnell JV, Siddiqui WA. 1972. The Effects of Antibiotics on 14C-isoleucine Incorporation by  
631 Monkey Erythrocytes Infected with Malarial Parasites. *Proceedings of the Helminthological  
632 Society of Washington* 39:201-203.
- 633 26. Tischer C, Hilsenstein V, Hanson K, Pepperkok R. 2014. Chapter 26 - Adaptive fluorescence  
634 microscopy by online feedback image analysis, p 489-503. *In* Waters JC, Wittman T (ed),  
635 *Methods in Cell Biology*, vol 123. Academic Press.
- 636 27. Carpenter AE, Jones TR, Lamprecht MR, Clarke C, Kang IH, Friman O, Guertin DA, Chang JH,  
637 Lindquist RA, Moffat J, Golland P, Sabatini DM. 2006. CellProfiler: image analysis software for  
638 identifying and quantifying cell phenotypes. *Genome Biol* 7:R100.
- 639 28. Ekong RM, Kirby GC, Patel G, Phillipson JD, Warhurst DC. 1990. Comparison of the in vitro  
640 activities of quassinoids with activity against *Plasmodium falciparum*, anisomycin and some  
641 other inhibitors of eukaryotic protein synthesis. *Biochemical pharmacology* 40:297-301.
- 642 29. Otoguro K, Ui H, Ishiyama A, Kobayashi M, Togashi H, Takahashi Y, Masuma R, Tanaka H,  
643 Tomoda H, Yamada H, Omura S. 2003. In vitro and in vivo antimalarial activities of a non-  
644 glycosidic 18-membered macrolide antibiotic, borrelidin, against drug-resistant strains of  
645 *Plasmodia*. *J Antibiot (Tokyo)* 56:727-9.
- 646 30. Keller TL, Zocco D, Sundrud MS, Hendrick M, Edenius M, Yum J, Kim Y-J, Lee H-K, Cortese JF,  
647 Wirth DF, Dignam JD, Rao A, Yeo C-Y, Mazitschek R, Whitman M. 2012. Halofuginone and other  
648 febrifugine derivatives inhibit prolyl-tRNA synthetase. *Nature Chemical Biology* 8:311-317.
- 649 31. Matthews H, Usman-Idris M, Khan F, Read M, Nirmalan N. 2013. Drug repositioning as a route to  
650 anti-malarial drug discovery: preliminary investigation of the in vitro anti-malarial efficacy of  
651 emetine dihydrochloride hydrate. *Malaria Journal* 12:359.

- 652 32. Reynolds JM, El Bissati K, Brandenburg J, Günzl A, Mamoun CB. 2007. Antimalarial activity of the  
653 anticancer and proteasome inhibitor bortezomib and its analog ZL3B. BMC clinical pharmacology  
654 7:13-13.
- 655 33. Crary JL, Haldar K. 1992. Brefeldin A inhibits protein secretion and parasite maturation in the  
656 ring stage of *Plasmodium falciparum*. Molecular and Biochemical Parasitology 53:185-192.
- 657 34. Andrews KT, Walduck A, Kelso MJ, Fairlie DP, Saul A, Parsons PG. 2000. Anti-malarial effect of  
658 histone deacetylation inhibitors and mammalian tumour cytodifferentiating agents. Int J  
659 Parasitol 30:761-8.
- 660 35. Fang P, Yu X, Jeong SJ, Miranda A, Chen K, Chen X, Kim S, Francklyn CS, Guo M. 2015. Structural  
661 basis for full-spectrum inhibition of translational functions on a tRNA synthetase. Nature  
662 Communications 6:6402.
- 663 36. Novoa EM, Camacho N, Tor A, Wilkinson B, Moss S, Marín-García P, Azcárate IG, Bautista JM,  
664 Miranda AC, Francklyn CS, Varon S, Royo M, Cortés A, Ribas de Pouplana L. 2014. Analogs of  
665 natural aminoacyl-tRNA synthetase inhibitors clear malaria in vivo. Proceedings of the National  
666 Academy of Sciences 111:E5508.
- 667 37. Herman JD, Pepper LR, Cortese JF, Estiu G, Galinsky K, Zuzarte-Luis V, Derbyshire ER, Ribacke U,  
668 Lukens AK, Santos SA, Patel V, Clish CB, Sullivan WJ, Jr., Zhou H, Bopp SE, Schimmel P, Lindquist  
669 S, Clardy J, Mota MM, Keller TL, Whitman M, Wiest O, Wirth DF, Mazitschek R. 2015. The  
670 cytoplasmic prolyl-tRNA synthetase of the malaria parasite is a dual-stage target of febrifugine  
671 and its analogs. Sci Transl Med 7:288ra77.
- 672 38. Wong W, Bai X-c, Brown A, Fernandez IS, Hanssen E, Condron M, Tan YH, Baum J, Scheres SHW.  
673 2014. Cryo-EM structure of the *Plasmodium falciparum* 80S ribosome bound to the anti-  
674 protozoan drug emetine. eLife 3:e03080.
- 675 39. Liaoo L-L, Kupchan SM, Horwitz SB. 1976. Mode of Action of the Antitumor Compound  
676 Bruceantin, an Inhibitor of Protein Synthesis. Molecular Pharmacology 12:167.
- 677 40. Sridhar S, Bhat G, Guruprasad K. 2013. Analysis of bortezomib inhibitor docked within the  
678 catalytic subunits of the *Plasmodium falciparum* 20S proteasome. SpringerPlus 2:566-566.
- 679 41. Yoshida M, Kijima M, Akita M, Beppu T. 1990. Potent and specific inhibition of mammalian  
680 histone deacetylase both in vivo and in vitro by trichostatin A. Journal of Biological Chemistry  
681 265:17174-17179.
- 682 42. Benting J, Mattei D, Lingelbach K. 1994. Brefeldin A inhibits transport of the glycophorin-binding  
683 protein from *Plasmodium falciparum* into the host erythrocyte. Biochem J 300 ( Pt 3):821-6.
- 684 43. Hanson KK, Ressurreicao AS, Buchholz K, Prudencio M, Herman-Ornelas JD, Rebelo M, Beatty  
685 WL, Wirth DF, Hanscheid T, Moreira R, Marti M, Mota MM. 2013. Torins are potent antimalarials  
686 that block replenishment of *Plasmodium* liver stage parasitophorous vacuole membrane  
687 proteins. Proc Natl Acad Sci U S A 110:E2838-47.
- 688 44. Delves M, Plouffe D, Scheurer C, Meister S, Wittlin S, Winzeler EA, Sinden RE, Leroy D. 2012. The  
689 Activities of Current Antimalarial Drugs on the Life Cycle Stages of *Plasmodium*: A Comparative  
690 Study with Human and Rodent Parasites. PLOS Medicine 9:e1001169.
- 691 45. LaMonte GM, Rocamora F, Marapana DS, Gnädig NF, Ottilie S, Luth MR, Worgall TS, Goldgof  
692 GM, Mohunlal R, Santha Kumar TR, Thompson JK, Vigil E, Yang J, Hutson D, Johnson T, Huang J,  
693 Williams RM, Zou BY, Cheung AL, Kumar P, Egan TJ, Lee MCS, Siegel D, Cowman AF, Fidock DA,  
694 Winzeler EA. 2020. Pan-active imidazolopiperazine antimalarials target the *Plasmodium*  
695 *falciparum* intracellular secretory pathway. Nature Communications 11:1780.
- 696 46. LaMonte G, Lim MY-X, Wree M, Reimer C, Nachon M, Corey V, Gedeck P, Plouffe D, Du A,  
697 Figueroa N, Yeung B, Bifani P, Winzeler EA, Wellems TE. 2016. Mutations in the *Plasmodium*  
698 *falciparum* Cyclic Amine Resistance Locus (PfCARL) Confer Multidrug Resistance. mBio 7:e00696-  
699 16.

- 700 47. Nixon GL, Moss DM, Shone AE, Lalloo DG, Fisher N, O'Neill PM, Ward SA, Biagini GA. 2013.  
701 Antimalarial pharmacology and therapeutics of atovaquone. *The Journal of antimicrobial*  
702 *chemotherapy* 68:977-985.
- 703 48. Phillips MA, Lotharius J, Marsh K, White J, Dayan A, White KL, Njoroge JW, El Mazouni F, Lao Y,  
704 Kokkonda S, Tomchick DR, Deng X, Laird T, Bhatia SN, March S, Ng CL, Fidock DA, Wittlin S,  
705 Lafuente-Monasterio M, Benito FJG, Alonso LMS, Martinez MS, Jimenez-Diaz MB, Bazaga SF,  
706 Angulo-Barturen I, Haselden JN, Louttit J, Cui Y, Sridhar A, Zeeman A-M, Kocken C, Sauerwein R,  
707 Dechering K, Avery VM, Duffy S, Delves M, Sinden R, Ruecker A, Wickham KS, Rochford R,  
708 Gahagen J, Iyer L, Riccio E, Mirsalis J, Bathhurst I, Rueckle T, Ding X, Campo B, Leroy D, Rogers  
709 MJ, et al. 2015. A long-duration dihydroorotate dehydrogenase inhibitor (DSM265) for  
710 prevention and treatment of malaria. *Science Translational Medicine* 7:296ra111.
- 711 49. Paquet T, Manach CL, Cabrera DG, Younis Y, Henrich PP, Abraham TS, Lee MCS, Basak R,  
712 Ghidelli-Disse S, Lafuente-Monasterio MJ, Bantscheff M, Ruecker A, Blagborough AM,  
713 Zakutansky SE, Zeeman A-M, White KL, Shackelford DM, Mannila J, Morizzi J, Scheurer C,  
714 Angulo-Barturen I, Martínez MS, Ferrer S, Sanz LM, Gamo FJ, Reader J, Botha M, Dechering KJ,  
715 Sauerwein RW, Tungtaeng A, Vanachayangkul P, Lim CS, Burrows J, Witty MJ, Marsh KC,  
716 Bodenreider C, Rochford R, Solapure SM, Jiménez-Díaz MB, Wittlin S, Charman SA, Donini C,  
717 Campo B, Birkholtz L-M, Hanson KK, Drewes G, Kocken CHM, Delves MJ, Leroy D, Fidock DA, et  
718 al. 2017. Antimalarial efficacy of MMV390048, an inhibitor of *Plasmodium*  
719 phosphatidylinositol 4-kinase. *Science Translational Medicine* 9:eaad9735.
- 720 50. Falco EA, Goodwin LG, Hitchings GH, Rollo IM, Russell PB. 1951. 2:4-diaminopyrimidines- a new  
721 series of antimalarials. *British journal of pharmacology and chemotherapy* 6:185-200.
- 722 51. Yuthavong Y, Tarnchompoo B, Vilaivan T, Chitnumsub P, Kamchonwongpaisan S, Charman SA,  
723 McLennan DN, White KL, Vivas L, Bongard E, Thongphanchang C, Taweekhai S, Vanichtanankul J,  
724 Rattanajak R, Arwon U, Fantauzzi P, Yuvaniyama J, Charman WN, Matthews D. 2012. Malarial  
725 dihydrofolate reductase as a paradigm for drug development against a resistance-compromised  
726 target. *Proceedings of the National Academy of Sciences of the United States of America*  
727 109:16823-16828.
- 728 52. Hounkpatin AB, Kreidenweiss A, Held J. 2019. Clinical utility of tafenoquine in the prevention of  
729 relapse of *Plasmodium vivax* malaria: a review on the mode of action and emerging trial data.  
730 *Infection and drug resistance* 12:553-570.
- 731 53. Foley M, Tilley L. 1998. Quinoline Antimalarials: Mechanisms of Action and Resistance and  
732 Prospects for New Agents. *Pharmacology & Therapeutics* 79:55-87.
- 733 54. Wong W, Bai XC, Sleebs BE, Triglia T, Brown A, Thompson JK, Jackson KE, Hanssen E, Marapana  
734 DS, Fernandez IS, Ralph SA, Cowman AF, Scheres SHW, Baum J. 2017. Mefloquine targets the  
735 *Plasmodium falciparum* 80S ribosome to inhibit protein synthesis. *Nat Microbiol* 2:17031.
- 736 55. Rankin KE, Graewe S, Heussler VT, Stanway RR. 2010. Imaging liver-stage malaria parasites.  
737 *Cellular Microbiology* 12:569-579.
- 738 56. Leiriao P, Mota MM, Rodriguez A. 2005. Apoptotic Plasmodium-Infected Hepatocytes Provide  
739 Antigens to Liver Dendritic Cells. *The Journal of Infectious Diseases* 191:1576-1581.
- 740 57. Grollman AP, Walsh WttaoM. 1967. Inhibitors of Protein Biosynthesis: II. MODE OF ACTION OF  
741 ANISOMYCIN. *Journal of Biological Chemistry* 242:3226-3233.
- 742 58. Jackson KE, Habib S, Frugier M, Hoen R, Khan S, Pham JS, Ribas de Pouplana L, Royo M, Santos  
743 MA, Sharma A, Ralph SA. 2011. Protein translation in *Plasmodium* parasites. *Trends Parasitol*  
744 27:467-76.
- 745 59. Hollien J. 2013. Evolution of the unfolded protein response. *Biochimica et Biophysica Acta (BBA)*  
746 - *Molecular Cell Research* 1833:2458-2463.

- 747 60. Meister S, Plouffe DM, Kuhen KL, Bonamy GMC, Wu T, Barnes SW, Bopp SE, Borboa R, Bright AT,  
748 Che J, Cohen S, Dharia NV, Gagaring K, Gettayacamin M, Gordon P, Groessler T, Kato N, Lee MCS,  
749 McNamara CW, Fidock DA, Nagle A, Nam T-g, Richmond W, Roland J, Rottmann M, Zhou B,  
750 Froissard P, Glynne RJ, Mazier D, Sattabongkot J, Schultz PG, Tuntland T, Walker JR, Zhou Y,  
751 Chatterjee A, Diagana TT, Winzeler EA. 2011. Imaging of Plasmodium liver stages to drive next-  
752 generation antimalarial drug discovery. *Science (New York, NY)* 334:1372-1377.
- 753 61. Kumar N, Koski G, Harada M, Aikawa M, Zheng H. 1991. Induction and localization of  
754 Plasmodium falciparum stress proteins related to the heat shock protein 70 family. *Molecular*  
755 *and Biochemical Parasitology* 48:47-58.
- 756 62. Kaiser G, De Niz M, Zuber B, Burda P-C, Kornmann B, Heussler VT, Stanway RR. 2016. High  
757 resolution microscopy reveals an unusual architecture of the Plasmodium berghei endoplasmic  
758 reticulum. *Molecular Microbiology* 102:775-791.
- 759 63. Gosline SJC, Nascimento M, McCall L-I, Zilberstein D, Thomas DY, Matlashewski G, Hallett M.  
760 2011. Intracellular Eukaryotic Parasites Have a Distinct Unfolded Protein Response. *PLOS ONE*  
761 6:e19118.
- 762 64. Ward P, Equinet L, Packer J, Doerig C. 2004. Protein kinases of the human malaria parasite  
763 Plasmodium falciparum: the kinome of a divergent eukaryote. *BMC genomics* 5:79-79.
- 764 65. Zhang M, Gallego-Delgado J, Fernandez-Arias C, Waters NC, Rodriguez A, Tsuji M, Wek RC,  
765 Nussenzweig V, Sullivan WJ, Jr. 2017. Inhibiting the Plasmodium eIF2alpha Kinase PK4 Prevents  
766 Artemisinin-Induced Latency. *Cell Host Microbe* 22:766-776 e4.
- 767 66. Bridgford JL, Xie SC, Cobbold SA, Pasaje CFA, Herrmann S, Yang T, Gillett DL, Dick LR, Ralph SA,  
768 Dogovski C, Spillman NJ, Tilley L. 2018. Artemisinin kills malaria parasites by damaging proteins  
769 and inhibiting the proteasome. *Nat Commun* 9:3801.
- 770 67. Zhang M, Mishra S, Sakthivel R, Rojas M, Ranjan R, Sullivan WJ, Fontoura BMA, Ménard R, Dever  
771 TE, Nussenzweig V. 2012. PK4, a eukaryotic initiation factor 2 $\alpha$ (eIF2 $\alpha$ ) kinase, is essential for the  
772 development of the erythrocytic cycle of Plasmodium. *Proceedings of the National*  
773 *Academy of Sciences* 109:3956-3961.
- 774 68. Axten JM, Medina JR, Feng Y, Shu A, Romeril SP, Grant SW, Li WHH, Heerding DA, Minthorn E,  
775 Mencken T, Atkins C, Liu Q, Rabindran S, Kumar R, Hong X, Goetz A, Stanley T, Taylor JD, Sigethy  
776 SD, Tomberlin GH, Hassell AM, Kahler KM, Shewchuk LM, Gampe RT. 2012. Discovery of 7-  
777 Methyl-5-(1-([3-(trifluoromethyl)phenyl]acetyl)-2,3-dihydro-1H-indol-5-yl)-7H-pyrrolo[2,3-  
778 d]pyrimidin-4-amine (GSK2606414), a Potent and Selective First-in-Class Inhibitor of Protein  
779 Kinase R (PKR)-like Endoplasmic Reticulum Kinase (PERK). *Journal of Medicinal Chemistry*  
780 55:7193-7207.
- 781 69. Obeng EA, Carlson LM, Gutman DM, Harrington WJ, Jr., Lee KP, Boise LH. 2006. Proteasome  
782 inhibitors induce a terminal unfolded protein response in multiple myeloma cells. *Blood*  
783 107:4907-16.
- 784 70. Van Voorhis WC, Adams JH, Adelfio R, Ah Yong V, Akabas MH, Alano P, Alday A, Alemán Resto Y,  
785 Alsibae A, Alzualde A, Andrews KT, Avery SV, Avery VM, Ayong L, Baker M, Baker S, Ben  
786 Mamoun C, Bhatia S, Bickle Q, Bounaadja L, Bowling T, Bosch J, Boucher LE, Boyom FF, Brea J,  
787 Brennan M, Burton A, Caffrey CR, Camarda G, Carrasquilla M, Carter D, Belen Cassera M, Chih-  
788 Chien Cheng K, Chindaoudomsate W, Chubb A, Colon BL, Colón-López DD, Corbett Y, Crowther GJ,  
789 Cowan N, D'Alessandro S, Le Dang N, Delves M, DeRisi JL, Du AY, Duffy S, Abd El-Salam El-Sayed  
790 S, Ferdig MT, Fernández Robledo JA, Fidock DA, et al. 2016. Open Source Drug Discovery with  
791 the Malaria Box Compound Collection for Neglected Diseases and Beyond. *PLOS Pathogens*  
792 12:e1005763.

- 793 71. Luth MR, Gupta P, Otilie S, Winzeler EA. 2018. Using in Vitro Evolution and Whole Genome  
794 Analysis To Discover Next Generation Targets for Antimalarial Drug Discovery. *ACS Infect Dis*  
795 4:301-314.
- 796 72. Okombo J, Kanai M, Deni I, Fidock DA. 2021. Genomic and Genetic Approaches to Studying  
797 Antimalarial Drug Resistance and Plasmodium Biology. *Trends Parasitol* 37:476-492.
- 798 73. Paquet T, Le Manach C, Cabrera DG, Younis Y, Henrich PP, Abraham TS, Lee MCS, Basak R,  
799 Ghidelli-Disse S, Lafuente-Monasterio MJ, Bantscheff M, Ruecker A, Blagborough AM,  
800 Zakutansky SE, Zeeman AM, White KL, Shackelford DM, Mannila J, Morizzi J, Scheurer C, Angulo-  
801 Barturen I, Martinez MS, Ferrer S, Sanz LM, Gamo FJ, Reader J, Botha M, Dechering KJ,  
802 Sauerwein RW, Tungtaeng A, Vanachayangkul P, Lim CS, Burrows J, Witty MJ, Marsh KC,  
803 Bodenreider C, Rochford R, Solapure SM, Jimenez-Diaz MB, Wittlin S, Charman SA, Donini C,  
804 Campo B, Birkholtz LM, Hanson KK, Drewes G, Kocken CHM, Delves MJ, Leroy D, Fidock DA, et al.  
805 2017. Antimalarial efficacy of MMV390048, an inhibitor of Plasmodium phosphatidylinositol 4-  
806 kinase. *Sci Transl Med* 9.
- 807 74. Dziekan JM, Yu H, Chen D, Dai L, Wirjanata G, Larsson A, Prabhu N, Sobota RM, Bozdech Z,  
808 Nordlund P. 2019. Identifying purine nucleoside phosphorylase as the target of quinine using  
809 cellular thermal shift assay. *Sci Transl Med* 11.
- 810 75. Forte B, Otilie S, Plater A, Campo B, Dechering KJ, Gamo FJ, Goldberg DE, Istvan ES, Lee M,  
811 Lukens AK, McNamara CW, Niles JC, Okombo J, Pasaje CFA, Siegel MG, Wirth D, Wyllie S, Fidock  
812 DA, Baragana B, Winzeler EA, Gilbert IH. 2021. Prioritization of Molecular Targets for  
813 Antimalarial Drug Discovery. *ACS Infect Dis* 7:2764-2776.
- 814 76. Lehane AM, Ridgway MC, Baker E, Kirk K. 2014. Diverse chemotypes disrupt ion homeostasis in  
815 the Malaria parasite. *Mol Microbiol* 94:327-39.
- 816 77. Allman EL, Painter HJ, Samra J, Carrasquilla M, Llinas M. 2016. Metabolomic Profiling of the  
817 Malaria Box Reveals Antimalarial Target Pathways. *Antimicrob Agents Chemother* 60:6635-6649.
- 818 78. Tamaki F, Fisher F, Milne R, Terán FS-R, Wiedemar N, Wrobel K, Edwards D, Baumann H, Gilbert  
819 IH, Baragana B, Baum J, Wyllie S. 2022. High-Throughput Screening Platform To Identify  
820 Inhibitors of Protein Synthesis with Potential for the Treatment of Malaria. *Antimicrobial Agents*  
821 *and Chemotherapy* 66:e00237-22.
- 822 79. Christophers SR, Fulton JD. 1939. Experiments with Isolated Malaria Parasites (Plasmodium  
823 Knowlesi) Free from Red Cells. *Annals of Tropical Medicine & Parasitology* 33:161-170.
- 824 80. Xie S, Griffin MDW, Winzeler EA, Ribas de Pouplana L, Tilley L. 2023. Targeting Aminoacyl tRNA  
825 Synthetases for Antimalarial Drug Development. *Annu Rev Microbiol* doi:10.1146/annurev-  
826 micro-032421-121210.
- 827 81. Ishiyama A, Iwatsuki M, Namatame M, Nishihara-Tsukashima A, Sunazuka T, Takahashi Y, Ōmura  
828 S, Otoguro K. 2011. Borrelidin, a potent antimalarial: stage-specific inhibition profile of  
829 synchronized cultures of Plasmodium falciparum. *The Journal of Antibiotics* 64:381-384.
- 830 82. Sugawara A, Tanaka T, Hirose T, Ishiyama A, Iwatsuki M, Takahashi Y, Otoguro K, Ōmura S,  
831 Sunazuka T. 2013. Borrelidin analogues with antimalarial activity: Design, synthesis and  
832 biological evaluation against Plasmodium falciparum parasites. *Bioorganic & Medicinal*  
833 *Chemistry Letters* 23:2302-2305.
- 834 83. Xie SC, Metcalfe RD, Dunn E, Morton CJ, Huang S-C, Puhlovich T, Du Y, Wittlin S, Nie S, Luth MR,  
835 Ma L, Kim M-S, Pasaje CFA, Kumpornsin K, Giannangelo C, Houghton FJ, Churchyard A,  
836 Famodimu MT, Barry DC, Gillett DL, Dey S, Kosasih CC, Newman W, Niles JC, Lee MCS, Baum J,  
837 Otilie S, Winzeler EA, Creek DJ, Williamson N, Parker MW, Brand S, Langston SP, Dick LR, Griffin  
838 MDW, Gould AE, Tilley L. 2022. Reaction hijacking of tyrosine tRNA synthetase as a new whole-  
839 of-life-cycle antimalarial strategy. *Science* 376:1074-1079.

- 840 84. Bhatt TK, Kapil C, Khan S, Jairajpuri MA, Sharma V, Santoni D, Silvestrini F, Pizzi E, Sharma A.  
841 2009. A genomic glimpse of aminoacyl-tRNA synthetases in malaria parasite *Plasmodium*  
842 *falciparum*. *BMC genomics* 10:644-644.
- 843 85. Jackson KE, Pham JS, Kwek M, De Silva NS, Allen SM, Goodman CD, McFadden GI, Ribas de  
844 Pouplana L, Ralph SA. 2012. Dual targeting of aminoacyl-tRNA synthetases to the apicoplast and  
845 cytosol in *Plasmodium falciparum*. *International Journal for Parasitology* 42:177-186.
- 846 86. Yu M, Kumar TRS, Nkrumah LJ, Coppi A, Retzlaff S, Li CD, Kelly BJ, Moura PA, Lakshmanan V,  
847 Freundlich JS, Valderramos J-C, Vilcheze C, Siedner M, Tsai JHC, Falkard B, Sidhu AbS, Purcell LA,  
848 Graud P, Kremer L, Waters AP, Schiehser G, Jacobus DP, Janse CJ, Ager A, Jacobs WR,  
849 Sacchettini JC, Heussler V, Sinnis P, Fidock DA. 2008. The Fatty Acid Biosynthesis Enzyme FabI  
850 Plays a Key Role in the Development of Liver-Stage Malarial Parasites. *Cell Host & Microbe*  
851 4:567-578.
- 852 87. Caicedo JC, Cooper S, Heigwer F, Warchal S, Qiu P, Molnar C, Vasilevich AS, Barry JD, Bansal HS,  
853 Kraus O, Wawer M, Paavolainen L, Herrmann MD, Rohban M, Hung J, Hennig H, Concannon J,  
854 Smith I, Clemons PA, Singh S, Rees P, Horvath P, Lington RG, Carpenter AE. 2017. Data-analysis  
855 strategies for image-based cell profiling. *Nat Methods* 14:849-863.
- 856 88. Vembar SS, Droll D, Scherf A. 2016. Translational regulation in blood stages of the malaria  
857 parasite *Plasmodium* spp.: systems-wide studies pave the way. *Wiley Interdiscip Rev RNA* 7:772-  
858 792.
- 859 89. Choi J-Y, Kumar V, Pachikara N, Garg A, Lawres L, Toh JY, Voelker DR, Ben Mamoun C. 2016.  
860 Characterization of *Plasmodium* phosphatidylserine decarboxylase expressed in yeast and  
861 application for inhibitor screening. *Molecular Microbiology* 99:999-1014.
- 862 90. Subramanian G, Belekar MA, Shukla A, Tong JX, Sinha A, Chu TTT, Kulkarni AS, Preiser PR, Reddy  
863 DS, Tan KSW, Shanmugam D, Chandramohanadas R, Sullivan WJ. 2018. Targeted Phenotypic  
864 Screening in *Plasmodium falciparum* and *Toxoplasma gondii* Reveals Novel Modes of Action of  
865 Medicines for Malaria Venture Malaria Box Molecules. *mSphere* 3:e00534-17.
- 866 91. Plouffe David M, Wree M, Du Alan Y, Meister S, Li F, Patra K, Lubar A, Okitsu Shinji L, Flannery  
867 Erika L, Kato N, Tanaseichuk O, Comer E, Zhou B, Kuhlen K, Zhou Y, Leroy D, Schreiber Stuart L,  
868 Scherer Christina A, Vinetz J, Winzeler Elizabeth A. 2016. High-Throughput Assay and Discovery  
869 of Small Molecules that Interrupt Malaria Transmission. *Cell Host & Microbe* 19:114-126.
- 870 92. Lucantoni L, Loganathan S, Avery VM. 2017. The need to compare: assessing the level of  
871 agreement of three high-throughput assays against *Plasmodium falciparum* mature  
872 gametocytes. *Scientific Reports* 7:45992.
- 873 93. Maher SP, Vantaux A, Chaumeau V, Chua ACY, Cooper CA, Andolina C, Péneau J, Rouillier M,  
874 Rizopoulos Z, Phal S, Piv E, Vong C, Phen S, Chhin C, Tat B, Ouk S, Doeurk B, Kim S, Suriyakan S,  
875 Kittiphanakun P, Awuku NA, Conway AJ, Jiang RHY, Russell B, Bifani P, Campo B, Nosten F,  
876 Witkowski B, Kyle DE. 2021. Probing the distinct chemosensitivity of *Plasmodium vivax* liver  
877 stage parasites and demonstration of 8-aminoquinoline radical cure activity in vitro. *Scientific*  
878 *Reports* 11:19905.
- 879 94. Allman EL, Painter HJ, Samra J, Carrasquilla M, Llinás M. 2016. Metabolomic Profiling of the  
880 Malaria Box Reveals Antimalarial Target Pathways. *Antimicrobial Agents and Chemotherapy*  
881 60:6635-6649.
- 882 95. Istvan ES, Guerra F, Abraham M, Huang KS, Rocamora F, Zhao H, Xu L, Pasaje C, Kumpornsin K,  
883 Luth MR, Cui H, Yang T, Palomo Diaz S, Gomez-Lorenzo MG, Qahash T, Mittal N, Otilie S, Niles J,  
884 Lee MCS, Llinas M, Kato N, Okombo J, Fidock DA, Schimmel P, Gamo FJ, Goldberg DE, Winzeler  
885 EA. 2023. Cytoplasmic isoleucyl tRNA synthetase as an attractive multistage antimalarial drug  
886 target. *Sci Transl Med* 15:eadc9249.

- 887 96. Prudencio M, Mota MM, Mendes AM. 2011. A toolbox to study liver stage malaria. Trends  
888 Parasitol 27:565-74.
- 889 97. Xie SC, Metcalfe RD, Dunn E, Morton CJ, Huang SC, Puhlovich T, Du Y, Wittlin S, Nie S, Luth MR,  
890 Ma L, Kim MS, Pasaje CFA, Kumpornsin K, Giannangelo C, Houghton FJ, Churchyard A, Famodimu  
891 MT, Barry DC, Gillett DL, Dey S, Kosasih CC, Newman W, Niles JC, Lee MCS, Baum J, Ottilie S,  
892 Winzeler EA, Creek DJ, Williamson N, Parker MW, Brand S, Langston SP, Dick LR, Griffin MDW,  
893 Gould AE, Tilley L. 2022. Reaction hijacking of tyrosine tRNA synthetase as a new whole-of-life-  
894 cycle antimalarial strategy. Science 376:1074-1079.
- 895 98. Valenciano AL, Gomez-Lorenzo MG, Vega-Rodriguez J, Adams JH, Roth A. 2022. In vitro models  
896 for human malaria: targeting the liver stage. Trends Parasitol 38:758-774.
- 897 99. Franke-Fayard B, Trueman H, Ramesar J, Mendoza J, van der Keur M, van der Linden R, Sinden  
898 RE, Waters AP, Janse CJ. 2004. A Plasmodium berghei reference line that constitutively  
899 expresses GFP at a high level throughout the complete life cycle. Mol Biochem Parasitol 137:23-  
900 33.
- 901 100. Tsuji M, Mattei D, Nussenzweig RS, Eichinger D, Zavala F. 1994. Demonstration of heat-shock  
902 protein 70 in the sporozoite stage of malaria parasites. Parasitology Research 80:16-21.
- 903 101. Trager W, Jensen JB. 1976. Human malaria parasites in continuous culture. Science 193:673-5.
- 904 102. Schindelin J, Arganda-Carreras I, Frise E, Kaynig V, Longair M, Pietzsch T, Preibisch S, Rueden C,  
905 Saalfeld S, Schmid B, Tinevez JY, White DJ, Hartenstein V, Eliceiri K, Tomancak P, Cardona A.  
906 2012. Fiji: an open-source platform for biological-image analysis. Nat Methods 9:676-82.
- 907 103. Berthold MR, Cebon N, Dill F, Gabriel TR, Kötter T, Meinel T, Ohl P, Sieb C, Thiel K, Wiswedel B.  
908 KNIME: The Konstanz Information Miner, p 319-326. *In* (ed), Springer Berlin Heidelberg,  
909

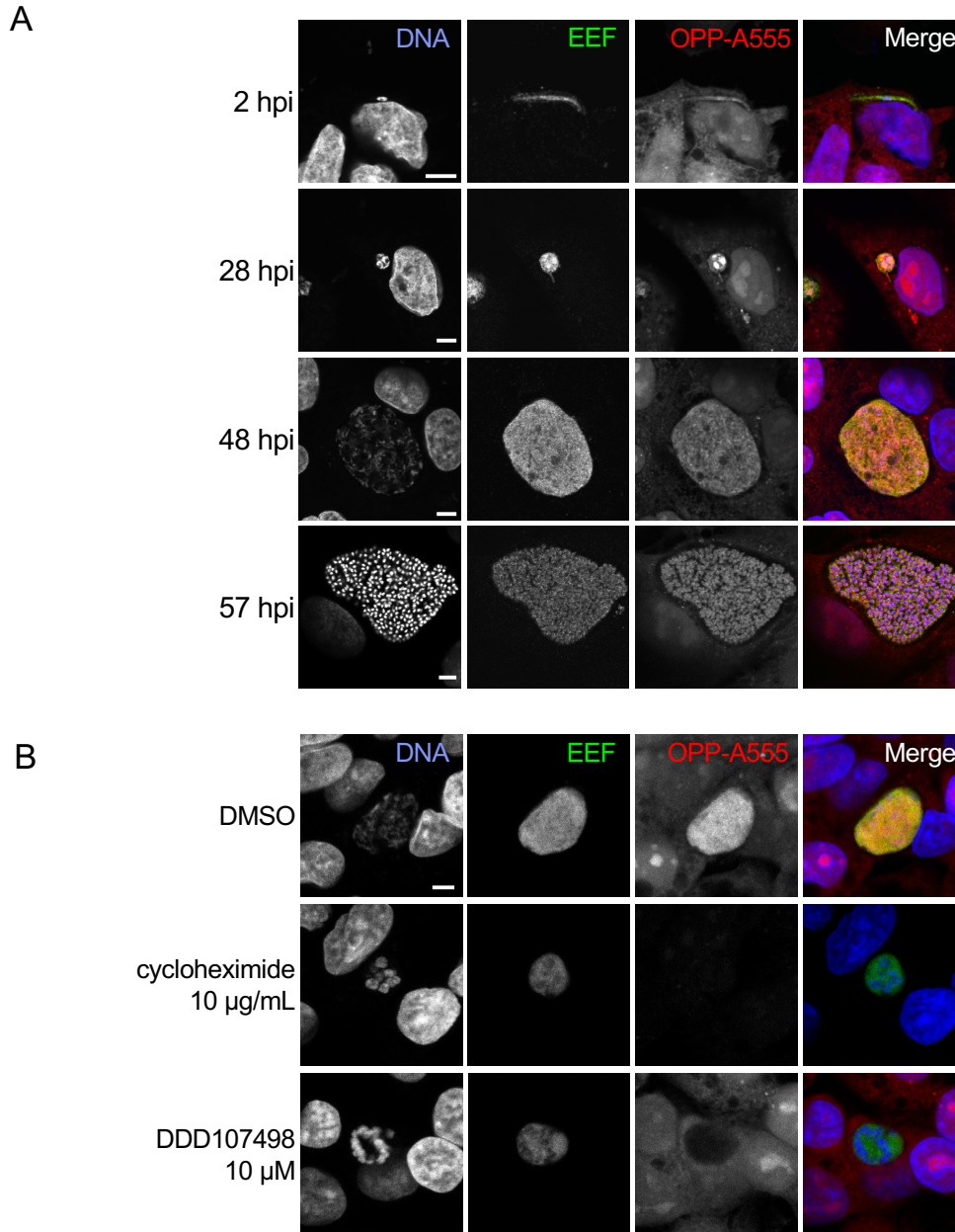
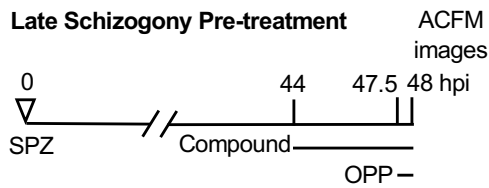
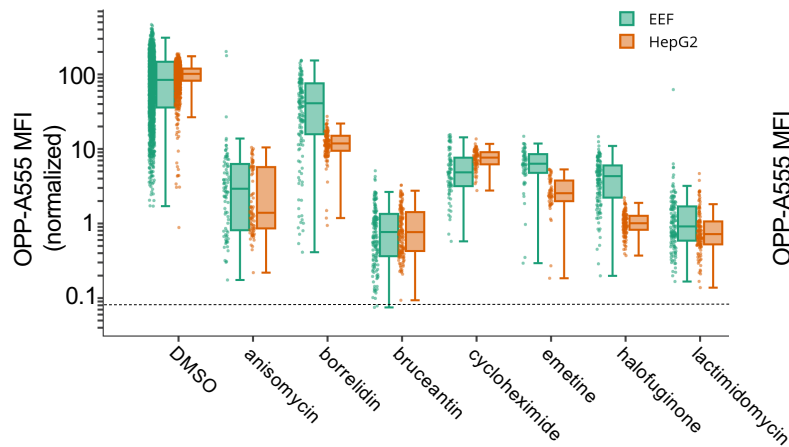


**Figure 1. Visualization of the nascent proteome in *Plasmodium berghei* liver stage parasites.** A-B) Representative, single confocal images of *P. berghei*-infected HepG2 cells, with OPP conjugated to Alexa Fluor 555 (OPP-A555) labeling the nascent proteome in both HepG2 and parasite (EEF), with Hoechst labeling DNA. Single channel images are shown in grayscale, with merges pseudo colored as labeled. A) Visualization of the nascent proteome throughout liver stage development, with parasite immunolabeled with  $\alpha$ -UIS4 (2 hpi) or  $\alpha$ -HSP70 (28, 48, and 57 hpi). B) Nascent proteome visualized in infected HepG2 cells following treatment from 44-48 hpi with translation inhibitors cycloheximide (10 µg/mL), or DDD107498 (10 µM) vs. DMSO control. All images in B) were acquired and processed with identical settings. Scale bars = 5 µm.

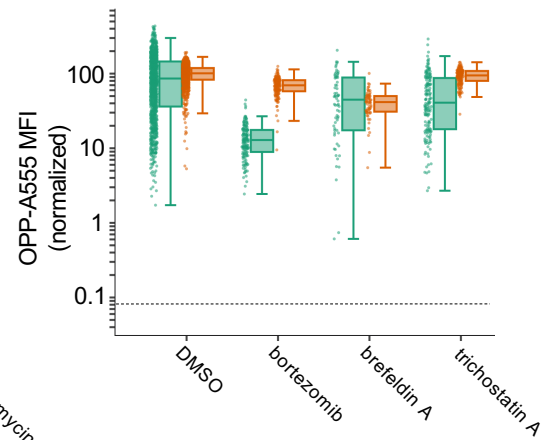
A



B



C



D

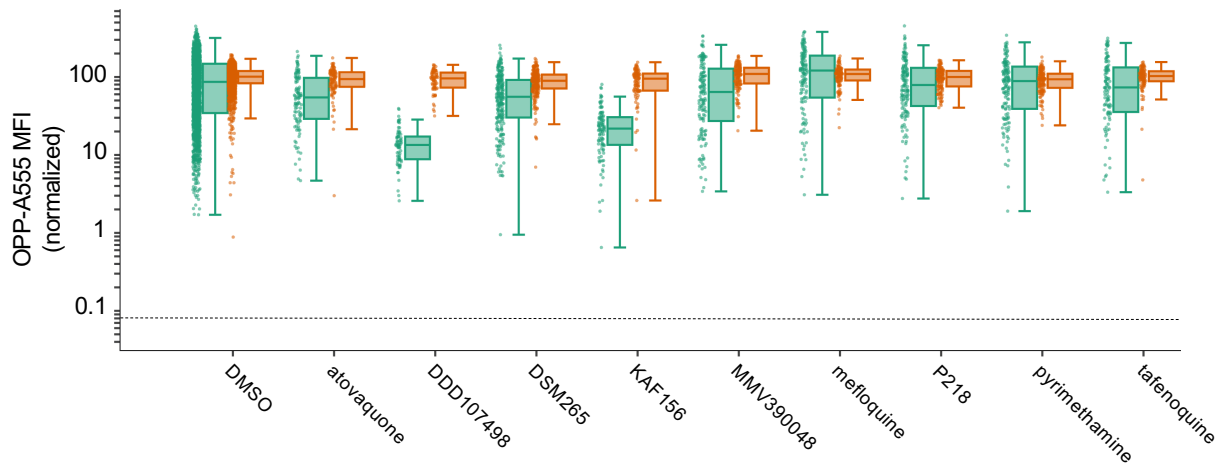


**Figure 2. Testing select bioactive compounds for inhibition of *Plasmodium* liver stage translation.**

Quantification of *P. berghei* and HepG2 protein synthesis after 3.5h pre-treatment with diverse, active compounds, as schematized in A). See Table S-1 for compound details. B-D) Boxplots quantifying translation inhibition via OPP-A555 mean fluorescence intensity (OPP-A555 MFI) from all single parasite ACFM images acquired for  $n \geq 3$  independent experiments, with each dot corresponding to a single EEF (green) or associated in-image HepG2 cells (orange). Specific signal cutoff (see Figure S2-3) is indicated by the dashed line. Compounds tested are known pan-eukaryotic translation inhibitors B), pan-eukaryotic inhibitors of cellular processes other than translation C), and antimalarial compounds D). Compounds were tested at 10  $\mu$ M except for cycloheximide (10  $\mu$ g/mL), tafenoquine (1.25  $\mu$ M), mefloquine (2.5  $\mu$ M), trichostatin A (5  $\mu$ M) & brefeldin A (5  $\mu$ g/mL).

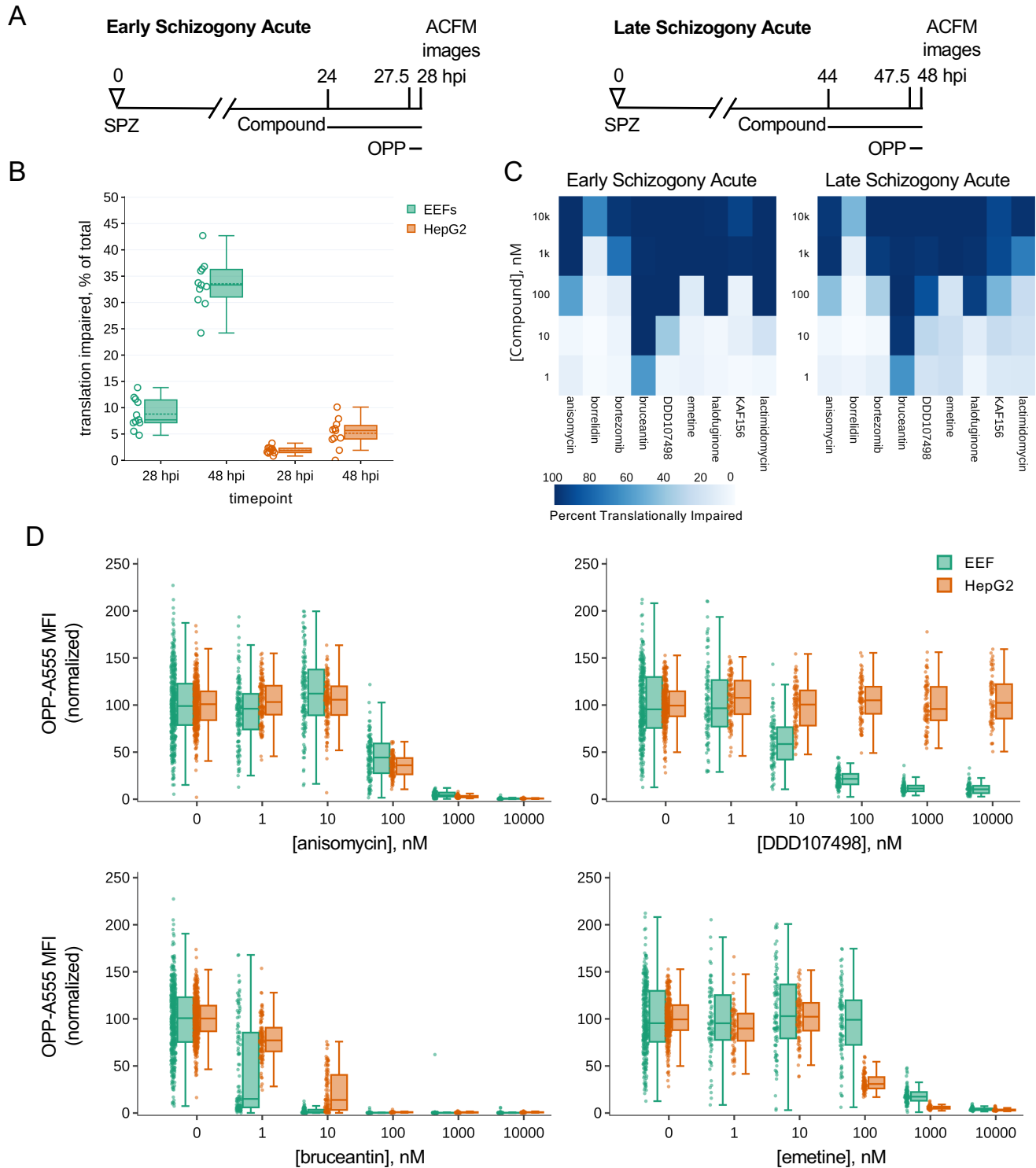


**Figure 3. Assessing heterogeneity and potency of translation inhibition during early and late schizogony.**

A) Experimental schematics. B) DMSO treated control EEFs and corresponding in-image HepG2 cells were classed as translationally impaired (individual parasite OPP-A555 MFI  $\leq$  50% of experiment OPP-A555 mean) or unimpaired during early and late schizogony; data show the mean of 11 matched independent experiments with circles representing individual experiment values. C-D) Determining potency of translation inhibition in *P. berghei* and in-image HepG2 cells after acute pre-treatment with the inhibitors identified in Fig. 2;  $n \geq 3$  independent experiments C) Percentage of single EEFs categorized as translationally impaired for inhibitors across concentrations in early and late schizogony. D) Concentration-response data in single parasites and in-image HepG2 cells for select translation inhibitors; all data normalized to mean of in-plate DMSO controls, set to 100.

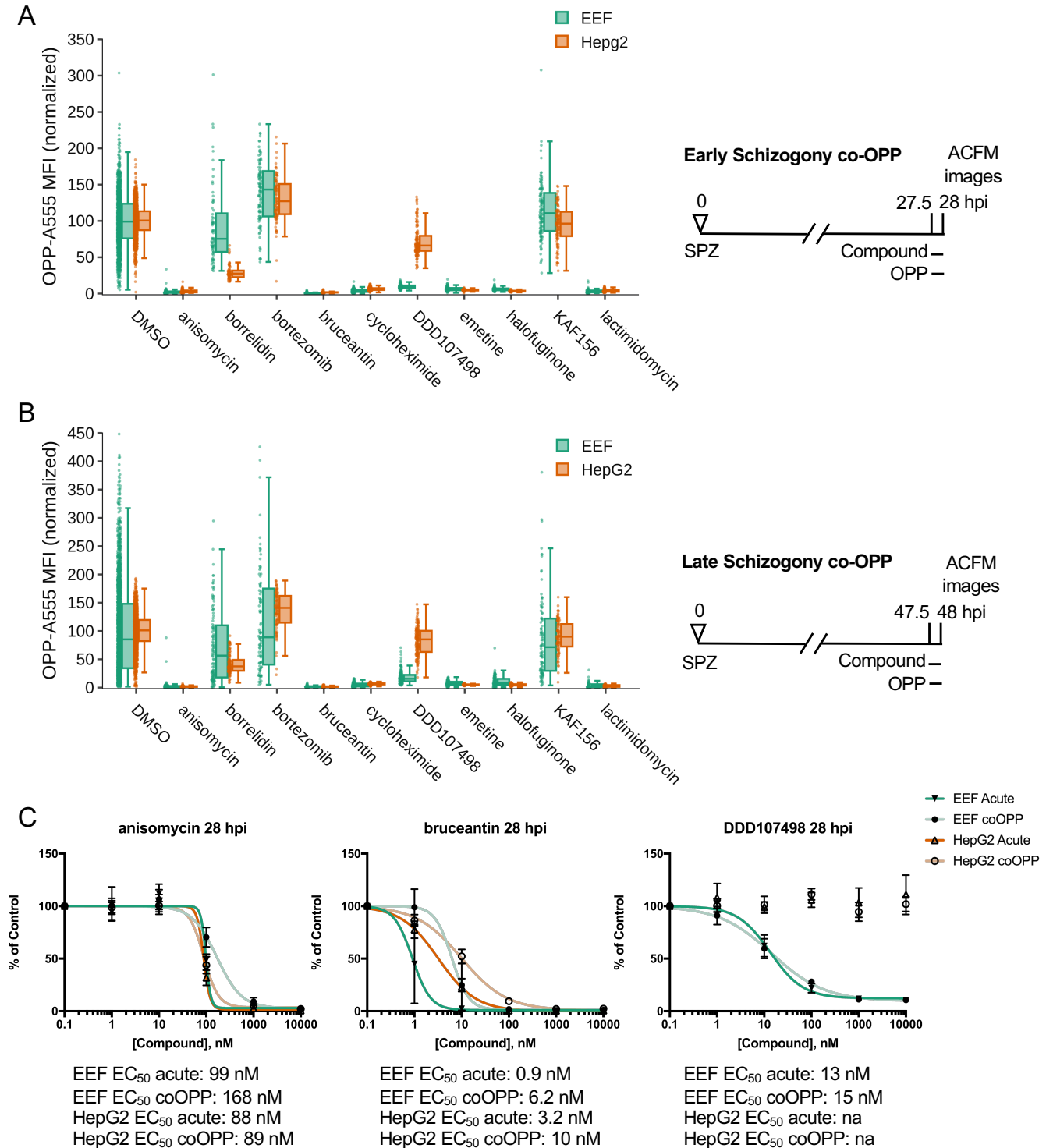


**Figure 4. Identification of direct vs. indirect translation inhibitors.** Quantification of protein synthesis in *P. berghei*-infected HepG2 cells in which active compounds at maximal concentrations were added together with OPP in early (A) and late (B) schizogony as described in figure schematics. Compound concentrations tested are the same as in Fig. 2. Each data point represents the normalized OPP-A555 mean fluorescence intensity (OPP-A555 MFI) of a single EEF or the corresponding HepG2 cells as labeled. C) Comparing coOPP and acute pre-treatment (from Fig. S3-1) concentration-response curves. All data shown was collected in  $n \geq 3$  independent experiments.

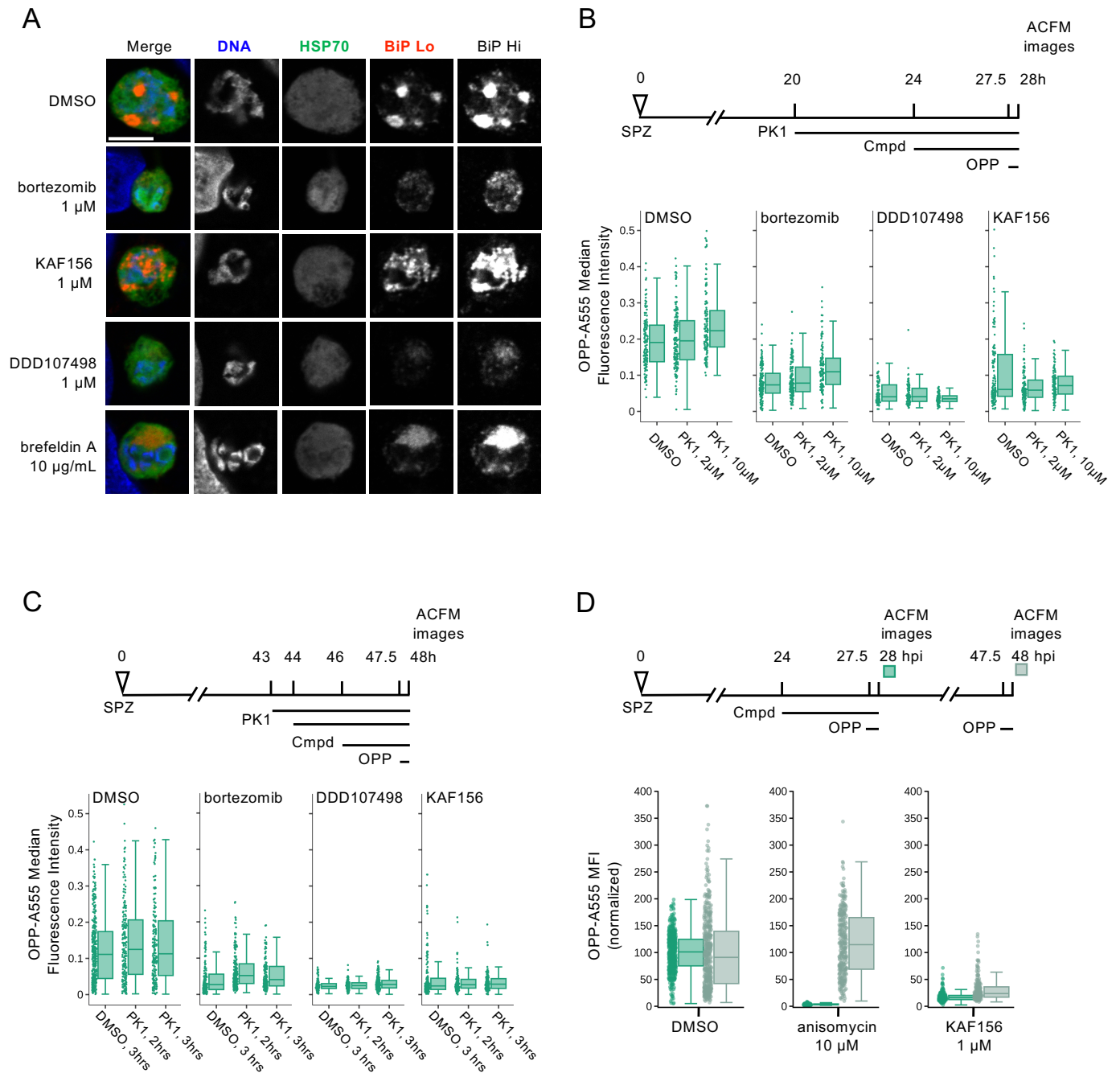


**Figure 5. Investigating the mechanism behind indirect translation inhibition.** A) Representative, single confocal images of *P. berghei* liver stage ER morphology after 4h compound treatment in early schizogony, at 28 hpi. Single channel images, all acquired with identical settings, are shown in grayscale, with merges pseudocolored as labeled; HSP70 marks the parasite and BiP specifically labels the parasite ER. Two images of BiP immunofluorescence were acquired with different gains (BiP Lo and BiP Hi) to visualize ER morphology across the range of BiP intensity observed. Scale bar = 5 $\mu$ m. B-D) Quantification of protein synthesis in single EEFs following treatments detailed in associated schematics. In B-C) [bortezomib] = 1  $\mu$ M, [KAF156] = 0.5  $\mu$ M, and [DDD107498] = 0.1  $\mu$ M were used to achieve similar levels of submaximal translational inhibition in the parasites.  $n \geq 3$  independent experiments. [PK1] as labelled in B), and 20  $\mu$ M in C). Data in D) was normalized to the mean of the DMSO control parasites for each timepoint.

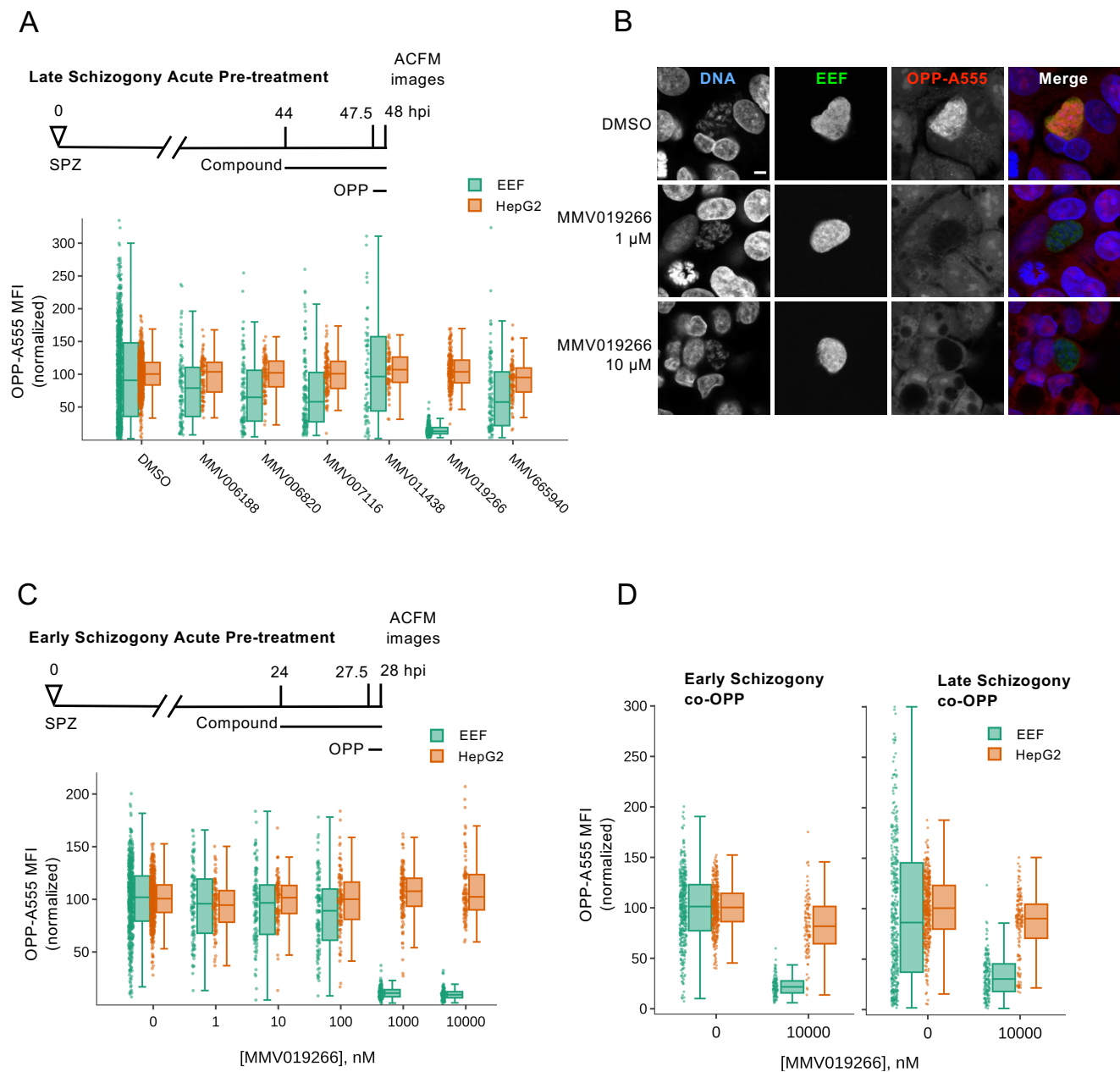


**Figure 6. Characterization of MMV019266 inhibition of *P. berghei* liver stage translation.** A) Select liver stage actives from the Malaria Box were tested at 10  $\mu$ M for ability to inhibit *P. berghei* liver stage translation following acute pre-treatment in late schizogony. B) Representative single confocal images of OPP-A55 labeling after 4h acute pre-treatments with MMV019266 vs. control in late schizogony; merges are pseudo colored as indicated with parasite (EEF) immunolabeled with  $\alpha$ -HSP70, and DNA stained with Hoechst. Scale bar = 5  $\mu$ m. C- D) Quantification of protein synthesis in *P. berghei*-infected HepG2 cells; compound treatments as described. Each data point represents OPP-A555 mean fluorescence intensity (MFI) normalized to in-plate controls;  $n \geq 3$  independent experiments.